AD-A261 970

(2)

# DOCUMENTATION PAGE

Form Approved
OMB No 0704-0188



| | |
|---|---|
| 1a. REPORT SECURITY CLASSIFICATION: Unclassified | 1b. RESTRICTIVE MARKINGS: None. |
| 2a. SECURITY CLASSIFICATION AUTHO[illegible] | 3. DISTRIBUTION/AVAILABILITY OF REPORT: Unlimited. |
| 2b. DECLASSIFICATION/DOWNGRADING [illegible]EDULE | |
| 4. PERFORMING ORGANIZATION REPORT NUMBER(S) | 5. MONITORING ORGANIZATION REPORT NUMBER(S) |
| 6a. NAME OF PERFORMING ORGANIZATION: Space Exploration Associates; 6b. OFFICE SYMBOL (If applicable) | 7a. NAME OF MONITORING ORGANIZATION: US Army Strategic Defense Comand |
| 6c. ADDRESS (City, State, and ZIP Code): PO Box 579, Cedarville, Oh 45314 | 7b. ADDRESS (City, State, and ZIP Code): CSSD-IM-PA, PO Box 1500, Huntsville AL 35807-3801 |
| 8a. NAME OF FUNDING/SPONSORING ORGANIZATION: SDIO; 8b. OFFICE SYMBOL (If applicable): T/IS | 9. PROCUREMENT INSTRUMENT IDENTIFICATION NUMBER: DASG60-92-C-0137 |
| 8c. ADDRESS (City, State, and ZIP Code): The Pentagon, Washington DC 20301-7100 | 10. SOURCE OF FUNDING NUMBERS: PROGRAM ELEMENT NO; PROJECT NO; TASK NO; WORK UNIT ACCESSION NO |

11. TITLE (Include Security Classification)
Joining CArbon Composite Fins to Titanium Heat Pipes

12. PERSONAL AUTHOR(S)
Elliot B Kennel, Arnold H. Deutchman, Robert L. Partyka, Anatoliy Yastrebkov, Yuri Nikolayev

| 13a. TYPE OF REPORT | 13b. TIME COVERED | 14. DATE OF REPORT (Year, Month, Day) | 15. PAGE COUNT |
|---|---|---|---|
| Final | FROM 92Jun08 TO 93Feb15 | 93Feb15 | |

16. SUPPLEMENTARY NOTATION

| 17. COSATI CODES | | | 18. SUBJECT TERMS (Continue on reverse if necessary and identify by block number) |
|---|---|---|---|
| FIELD | GROUP | SUB-GROUP | Titanium, heat pipe, diffusion bonding, carbon-carbon Ion Implantation, Ion Beam Enhanced Deposition (IBED). |
| | | | |
| | | | |

19. ABSTRACT (Continue on reverse if necessary and identify by block number)

An experimental effort was conducted to metallize a high thermal conductivity carbon carbon composite using ion beam enhanced deposition, and then to join it to titanium by diffusion bonding. Basic feasiblity of the concept was demonstrated.



| 20. DISTRIBUTION/AVAILABILITY OF ABSTRACT | 21. ABSTRACT SECURITY CLASSIFICATION | |
|---|---|---|
| ☒ UNCLASSIFIED/UNLIMITED ☐ SAME AS RPT ☐ OTIC USERS | Unclassified | |
| 22a. NAME OF RESPONSIBLE INDIVIDUAL | 22b. TELEPHONE (Include Area Code) | 22c. OFFICE SYMBOL |

# High Quality Joints Between Composite Fins and Metal Heat Pipes

**FINAL REPORT**

Elliot B. Kennel, Principal Investigator
Arnold H. Deutchman
Robert L. Partyka
Yuri V. Nikolayev
Anatoliy A. Yastrebov

Space Exploration Associates
PO Box 579
Cedarville Ohio 45314

BeamAlloy Corp
6360 Dublin Industrial Lane
Dublin Ohio 43017

## TABLE OF CONTENTS

## I. SUMMARY

This effort sought to explore the possibility of joining composite fins to metal using ion beams to modify the composite surface to more closely resemble the metal surface. The specific application targeted for this effort was forming thermally conductive fins for heat pipes. This will enable the use of exceptionally high thermal conductivity, low weight graphite composite fins with titanium heat pipes.

The basic concept is to create an exceptionally adherent interface zone using an ion-beam ballistic bonding technique to treat the surfaces of the materials to be joined. The interface material can be virtually any material which can form a plasma. It need not be metallurgically soluble with the substrate. For example, previous efforts have formed stable bonds of gold to molybdenum and even gold to rubber. Having created a metallic interface on the host composite (e.g., titanium), it is then possible to diffusion bond it to a piece of pure titanium or to another composite. Thus, the proposed technique would enable rigorously adherent, exceptionally strong bonds between materials which presently can not be joined. It is proposed to demonstrate this on carbon/carbon pieces.

Current state of the art is to try to braze or glue fins onto the heat pipe. However, there are limitations of this method. First, it is usually necessary to have a heat pipe/fin assembly which can withstand thermal cycling. Second, it is important to maintain excellent thermal conductance to avoid temperature drop in the joint. Third it is necessary to resist high temperature creep over seven to ten year life. Fourth it is necessary to withstand launch vibration. Thus, many DOD, DOE and NASA programs have sought to acquire the low mass benefits from using high thermal conductivity composite fins, but all of these programs have been less than satisfactory to date because of inadequate joining technology.

The effort was successful in that graded interfaces were produced between titanium and carbon carbon. These materials were successfully brazed. Lesser success was observed with diffusion bonding (which was the preferred technique due to the thinness of the joint). The two pieces stuck, but severe mismatches of thermal expansion were sufficient to break the joint in many of the samples.

Prior to the experiment we had assumed that the interface layer would be at least as strong as the surrounding material because of the strong bonding which results from injecting the titanium into the atomic lattice. However, this was not the case. At least, we were not able to overcome the thermal mismatch as we had hoped.

There are three possible reasons for this. First, it is possible that the carbon lattice was itself damaged or weakened by the ion injection process. This could occur if the $sp^2$ or $sp^3$ bonds in the lattice were preferentially destroyed and replaced with weaker bonds between carbon atoms. Second, it is possible that, during the diffusion bonding process, the titanium atoms in the carbon lattice were permitted to diffuse into lower energy states, thus weakening the interface zone. Third, it is possible that the surface of the carbon itself is weakened by cutting. Although we took steps to ensure that the surface was as clean as possible and polished flat, it could still be seen under a microscope that there were loose fibers and microcracks near the surface. It is possible, therefore, that the great strength

exhibited by carbon-carbon is truly a bulk property, and that near the surface it is much more brittle and weak on the microscopic level.

Our conclusion is that the basic feasibility of the proposed method has been established; however superior characteristics compared to other methods has not yet been demonstrated. Carbon-carbon may not have been the most favorable selection for the first demonstration of the technique.

## II. BACKGROUND

There are now exceptional carbon fibers which can be used to make composite materials with exceptionally high thermal conductivity. For instance, Applied Sciences Inc has pioneered the development of vapor grown graphite fiber or VGCF. This fiber is produced by decomposition of methane, and has a nearly single-crystal "onion skin" geometry, producing exceptional thermal conductivity in the axial direction, while maintain reasonable flexibility and strength. VGCF has an astounding thermal conductivity of 1900 W/mK at ambient temperature. This value is five times higher than that of copper, and nine times higher than that of aluminum. Furthermore, for space radiators, the true figure of merit is thermal conductivity divided by density. In composite form, fiber-containing composites have produced mass-normalized specific thermal conductivity in excess of 700 $(W/m\text{-}^{o}K)/(g/cm^3)$. This corresponds to a value of nine times that of aluminum and sixteen times that of copper.

Although some of the first composites produced had low strength, recent success with chemical vapor infiltration (CVI) has resulted in the production of exceptionally strong composites while retaining the excellent thermal properties of the carbon fiber. The CVI method is preferred because it requires very little handling of the fibers (and associated breaking and damaging of the fibers), thus preserving the highly conductive nature of the fiber. Thus it is reasonable to assume that a very strong carbon composite can be fabricated, which will afford structural stability and resistance to vibration, such as which might be encountered in the space launch environment.

Accordingly, several US firms have sought to exploit high thermal conductivity fins for spacecraft heat rejection apparatus, such as heat pipe/fin radiators. It is especially important to minimize the temperature drop in space radiators because of the inverse $T^4$ dependence of radiator area.

The "Achilles heel" for high conductivity composites is joining technology. Adhesives and brazes have been developed, but typically these joining techniques lack the strength and temperature resistance of the base material. Moreover, brazing generally results in a sharp interface zone at the joint where metallurgical and thermomechanical properties vary greatly. The disparity in the thermal expansion properties (linear and volumetric) of the materials at the joint can result in the production of interfacial stresses during temperature cycling which can result in joint failure. In addition, thermal energy transfer across the joint can be limited by the properties of the sharp interface zone.

For these reasons, composite fins and heat pipes are generally not compatible with state of the art joining techniques.

There are currently two important efforts in heat pipe/composite fin radiator development. These are being undertaken under the auspices of NASA Lewis Research

Center, partially with funding from SDIO.

The first, with Rocketdyne Division of Rockwell International, uses a carbon-carbon sandwich to encase a titanium heat pipe. Because of the rather complex weaving which is used, it is not possible to use VGCF or similar fibers for this project. In this case the joining problem is solved by relying on low performance (but highly workable) carbon fibers to fabricate the carbon-carbon sandwich. Accordingly, the manufacturability risk is low, but the performance achieved from the fins is not as high as it might be.

A second effort with Space Power Inc uses high performance carbon fiber fins, and a transition heat pipe is brazed onto the surface of the fin. Brazing onto the flat side of the heat pipe is simpler than a butt-joint, though of course from a weight standpoint it is not the most effective approach. If better, more reliable joining technology were available, it would be possible to design longer fins with less massive joints.

Other projects in the past have been less successful.

To join a carbon-carbon composite fin to a metal heat pipe, the concept is to use an ion beam technique (several such techniques exist as will be explained below), to ballistically bond a metallic interface zone on the joining surface of the fin. It will then be possible to the fin to the pipe with a metal to metal joining technique such as diffusion bonding.

Metal to metal joining is not nearly as challenging as composite to metal joining.

## III. ION BEAM TECHNIQUES

Ion beam techniques are currently in use to deposit materials such as tungsten carbide on steel machining tools (e.g., drill bits). The interface zone absolutely does not separate from the steel, but can only come off after abrasive action. The interface zone is much more resistant to abrasion than the bare metal, obviously. The technology is used extensively in the commercial sector, but has not received much attention yet in aerospace R & D.

Ion beam implantation techniques have come into increasingly common use in the past decade. Ion implantation is the process of introducing atoms of alloying elements into the surface layers of a solid material by accelerating the atoms to high energies (50 to 200 kilovolts) and allowing them to strike the surface of the material. The energetic ions penetrate into the surface of the material to depths ranging from 0.01 to 1 micron depending on the energy of the ion, thereby creating a thin, alloyed surface layer.

When the ions interact with the target atoms, two forms of energy loss occur. These are elastic scattering, and inelastic scattering. In the latter, interaction of the ion with the electrons of the target material atom causes the target atom to be displaced. If the displaced atom receives sufficient energy, it may cause additional displacements in a subsequent collision cascade. These additional displacements continue until no atom in the cascade has sufficient energy to cause displacements, generally in the range of 25 eV. In the region which encompasses heavy ion cascade, (1,000 to 10,000 atoms) between 10% and 100% of the atoms in the target may be displaced. The considerable rearrangement of atoms in the target is known as ballistic cascade mixing.

Since the atoms are implanted ballistically and not through thermal action, there is no need for the application of high temperatures. The host substrate can be kept at any

temperature during the process, as long as the waste heat from the ion beam is removed.

Graded interfaces, with maximum implanted atom concentrations at the surface of the implanted material can be produced with a variation of direct ion implantation termed ion beam mixing. In this process, a thin layer of one atomic species is deposited on the surface of the material to be implanted. A beam of chemically inert atoms (typically, argon or xenon are used) is then used to mix the overlayer into the substrate. Due to the highly concentrated source overlayer, ion beam mixing is not limited by sputtering effects, and the concentration of beam-mixed atoms on the substrate surface can approach 100 atomic weight percent. The concentration gradients and distribution profiles can be tailored by proper choice of beam mixing species, doses and energies. The absence of a discontinuous interface between the mixed surface layer and the bulk material leads to excellent adhesion of the layer and less sensitivity to mechanical failure at elevated temperatures and during thermal cycling.

Ion beam mixing can be used to produce layers of metallic or other materials which will grade continuously into the surface of C/C composites. For purposes of clarity, the numbers of atoms are greatly reduced, and a simple homogeneous array of atoms is depicted. Since there is distinct interface between the graded ion-beam mixed surface layer and the sub-surface of the C/C composite, interfacial stresses will be minimized during temperature cycling, and the mechanical stability of the surface layers will be increased, thereby eliminating cracking and spalling. The graded layer will also be bonded more effectively to the C/C surface since it is physically mixed into the composite surface. The result is an exceptionally strong bonded surface.

These ion implantation techniques can produce an excellent thin, adherent coating of metal or any material that can be made into a plasma on any substrate. The strong bond, coupled with the thinness of the coating, provides reasonable assurance that the coating will not come off during thermal cycling. The thinness of the coating and the exceptionally strong physical bond to the substrate surface prevents the coating from delaminating from the surface, even if there is a significant thermal expansion coefficient mismatch. Note that since the process is an ion bombardment process, it is possible to produce alloys or phases which do not exist in equilibrium.

The metallurgical structures formed on the surface of C/C composite materials using IBED is diagrammed in Figure 1. Pure titanium metal is initially alloyed into the surface of the C/C at atomic percentage concentrations in excess of 90%. This layer of titanium metal is graded into the C/C surface to a depth of

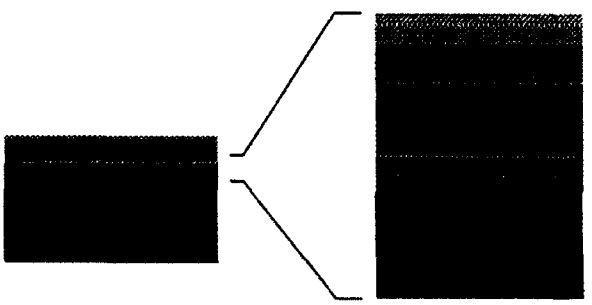

Figure 1 IBED coatings are alloyed directly into the surface of the C/C composite. Excellent adhesion is obtained since there is an actual physical mixing of the coating into the C/C surface. The presence of a graded interface zone minimizes the effects of stresses generated at this interface during thermal cycling because of the coefficient of thermal expansion mismatch between the C/C and the coating.

approximately 650 Angstroms. Once this graded interface is formed, the IBED process is used to grow a thicker layer of pure titanium metal out from the surface as a coating. Due to the action of the high energy ion beams, the titanium coating deposited is fully dense and compressively loaded thereby improving the adhesion and mechanical properties of the coating. This pure titanium metal coating forms the zone that is subsequently diffusion bonded to the titanium metal component of interest.

**Ion Beam Enhanced Deposition Process**

The IBED process utilized to deposit the coatings investigated in this work is outlined in Figure 2. Samples to be coated are mounted to a rotating, angling platen assembly located in a high vacuum processing chamber. Titanium metal is continuously deposited as an atomistic vapor onto the surface of the C/C samples via vacuum evaporation. An independently controllable, variable energy, inert gas (Argon) ion beam is used to simultaneously illuminate the titanium metal as it condenses on the C/C sample surface. In the initial phase of coating formation, the energy of the atoms in the Argon beam is set to mix the titanium into the C/C surface to form the graded junction in the surface. Once the proper titanium concentration is achieved in the surface, the energy of the atoms in the Argon beam is changed to allow the titanium coating to grow out from the surface. The exact metallurgical nature, and therefore the performance of the layer as a bond coat, will be determined by the specific deposition parameters used to form the layers.

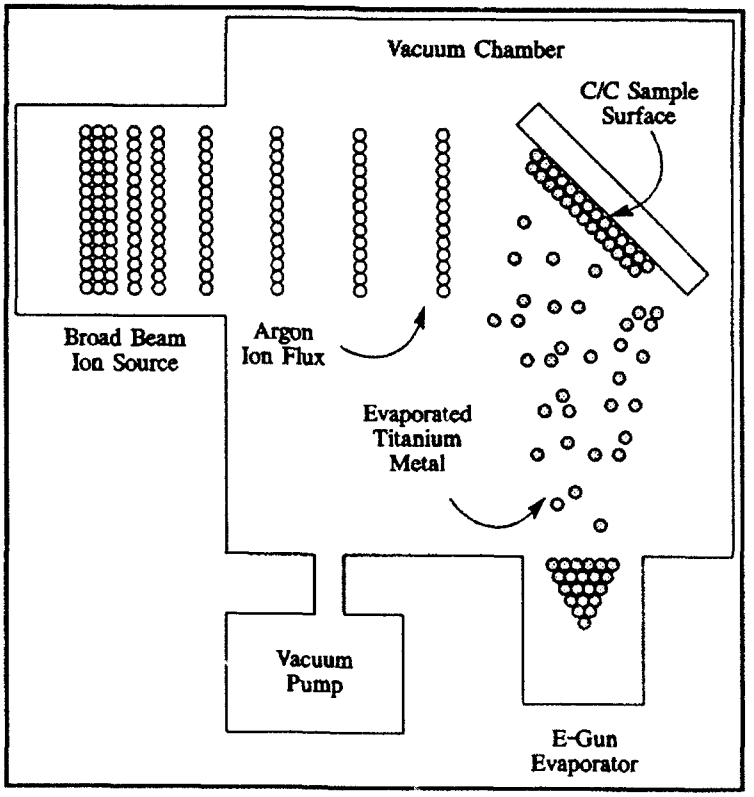


Figure 2 Ion Beam Enhanced Deposition Process

Carbon-carbon fins and titanium heat pipes were the first candidate system to be tried, because of the high payoff associated with carbon-carbon fins. Titanium was suggested as an initial candidate because of its oxidation resistance, good temperature capability ($T_{melt}$ = 2090 K), low coefficient of thermal expansion (5 x $10^{-6}$) high strength, creep resistance, compatibility with liquid metal working fluids, and the wide range of joining techniques which are available for this widely-used aerospace material. Other candidate metals include aluminum (for near-ambient temperature applications), nickel, stainless steel, niobium and perhaps molybdenum and alloys.

Ultimately, the temperature capability will probably be limited by the formation of TiC via diffusion of carbon into the titanium region, a process which is a function of time and temperature and which has been well characterized by Vansant and Phelps (1966) and Hollox (1969).[0,1] Based on this research, there should be no problem coexisting for many years at the 1000 K regime, but only hundreds of hours can be guaranteed above about 1500 K (of course, the titanium heat pipe itself will not be much good at such high temperatures anyway as it will have lost most of its strength). A reasonable operating point for a titanium/potassium heat pipe is probably in the range of 800-900 K, and carbon diffusion not be able to contact the working fluid for at least ten years, even if the pipe is very thin.

Note also that it is possible to obviate the problems caused by mismatches in the differential coefficient of expansion between different materials. Because ion beam techniques do not depend on the temperature of the substrate, it is possible to create the interface at an elevated temperature. This was not done during Phase I because of the expense of modifying the existing ion beam setup, but it will not be difficult to provide a high current feedthrough for a heater.

If a coated sample is heated to operating temperature during deposition, then it should be at the minimum internal stress point at that temperature. The titanium interface thus created will be in tension at ambient temperature, and relax (achieve near zero stress) as its operating temperature.

If the sample is kept at ambient during deposition (and this was the case for all samples during this effort, then the titanium interface is at minimum internal stress at ambient temperature. During heating to operating temperature, the titanium interface will be under compression.

If the sample is kept above operating temperature during deposition, then the titanium interface will be a minimum internal stress at high temperature. At operating temperature, the interface will be in tension at operating temperature, and severe tension at ambient. This is the condition created by virtually all other thermal joining techniques (brazing, welding, diffusion bonding, etc.).

This is expected to result in an excellent capability to withstand thermal cycling, thermal shock and to minimize the effects of thermal expansion coefficient mismatches within wide limits.

## IV. Experimental

Three different types of carbon-carbon were used for this effort. The first, from General Electric, was a standard low-cost construction grade carbon-carbon. It was selected because of its widespread use and low cost, which make it an excellent material for normal structural applications.

The second type, from SAIC, is similar in weave and structure to the carbon-carbon that they make using high thermal conductivity fiber. For instance, these carbon-carbon samples were used by SPI for their high performance radiator effort.

The third type, manufactured by Applied Sciences Inc., uses oriented high thermal conductivity vapor grown carbon fiber (VGCF) to produce very high thermal conductivity along the axis of the fin. This material achieved a thermal conductivity of 740 W/mK, by far the highest thermal conductivity of any material used in the study, and one of the highest thermal conductivity composites ever manufactured. Ultimately such composites may approach 1000 W/mK.

For the first trial, GE samples and SAIC samples were cut on a diamond saw and sent to BeamAlloy for processing. No additional preparation was made.

Using ion beam enhanced deposition, a coating of 0.5 microns was applied to the surface.

### IBED Protocol Development

Prior to ion beam enhanced deposition treatment, all carbon-carbon samples were cleaned ultrasonically in a solution of methanol or acetone.

Initial estimates of the optimum deposition protocols were made, and an initial sequence of trial deposition protocols were established. An initial series of three C/C samples sets were coated with IBED titanium layers, one with the optimum deposition protocol, and one each with a set of deposition protocols with higher and lower energy per deposited atom values. The adhesion of the titanium coatings deposited using each deposition protocol was evaluated by simple Scotch™ tape testing. On the basis of the results of the adhesion test, an additional set of C/C samples was coated using the "best" deposition protocols. The initial three sets of deposition protocols are listed in Table I.

**Table I. Initial Trial Deposition Protocols**

| Titanium Arrival Energy | | | Deposition Protocols | | |
|---|---|---|---|---|---|
| Protocol | Atom Number Ratio: Ti/Ar | Ti Atom Energy (eV) | Ti Evap. Rate (A/sec) | Argon Beam Energy (keV) | Argon Beam Current (mA) |
| High Collision Energy | 417 | 240 | 30 | 100 | 4 |
| Optimum Protocol | 417 | 120 | 30 | 50 | 4 |
| High Ti/Ar Ratio | 833 | 120 | 60 | 100 | 4 |

Each sample set consisted of six C/C samples. Two samples (General Electric) were cube-shaped, approximately 1 cm long on each side. The remaining four samples (SAIC carbon carbon) were shaped like cooling fins, 2 cm x 1 cm x 1 mm thick. One face of the cube-shaped samples, and the entire O.D. of one end of the fin-shaped samples was coated. The IBED coating deposited on all samples using all three deposition protocols was 5000 Angstroms (½ micron) thick.

After IBED deposition, the samples were examined optically and subjected to coating adhesion tests. In some cases, though the coating adhered to the graphite surface, the surface itself was only loosely bonded to the substrate. For example, individual strands of graphite could be seen seemingly to rest at the surface. When disturbed by an adhesion test, the graphitic strands sometimes pulled up off the surface.

**Coating Adhesion Test**

The coated surface of all samples appeared silvery in color, and the titanium coating did not delaminate under the rubbing action of a soft cloth. When the coated surfaces were rubbed across bond paper, carbon was transferred to the paper from the uncoated area but not from the coated area. The appearance of a typical IBED Titanium coated C/C sample surface is seen in Figure A-1 to A9.

A simple "Scotch™ tape test was performed to verify that the ion beam interface was adequately formed. This coating adhesion testing was performed by pressing Scotch™ tape on the coated surface of the C/C samples and observing the appearance of both the coated surface and the tape after the tape was pulled off. The results of the adhesion testing are tabulated in Table II.

**Table II Appearance of C/C and Scotch™ Tape Surfaces After Testing**

| Protocol | C/C Surface Uncoated | C/C Surface Coated | Tape - Uncoated Surface | Tape - Coated Surface |
|---|---|---|---|---|
| High Collision Energy | Black | Dull Metallic | High Density of Carbon Particles | Low Density of Carbon Particles |
| Optimum Protocol | Black | Dull Metallic | High Density of Carbon Particles | Low Density of Carbon Particles |
| High Ti/Ar Ratio | Black | Brighter Metallic | High Density of Carbon Particles | No Carbon Particles |

The High Ti/Ar Arrival Ratio deposition protocol produced IBED titanium coatings with the best adhesion. There was no delamination of the titanium coating from the coated surface. The IBED titanium coatings deposited with the other two deposition protocols delaminated at small spots in a random pattern all over the coated surface

Prior to coating, it was noticed that the surfaces of all C/C samples were contaminated with a black powdery residue. This residue was most likely small diameter graphite particles remaining from the cutting operations. Since this residue could influence the coating adhesion, especially as thicker layers are deposited, it was recommended that all samples be lapped after cutting to remove as much of the remnant cutting debris as possible.

**Deposition Of A 3 Micron Thick Layer**

The High Ti/Ar Arrival Ratio deposition protocol was used to coat an additional set of C/C samples. The samples were cut to shape with a diamond saw and then the surfaces to be coated were lapped smooth. Lapping was done first with 5 micron diameter alumina, and then with 1 micron diameter alumina. The lapped samples were then cleaned with methanol under ultrasonic agitation. After coating with a 3 micron thick IBED titanium layer the sample surfaces had a matte metallic appearance. Typical coated sample surfaces are shown in Figure A-15 to A-16.

The IBED coating is deposited uniformly across the surface of the C/C sample and replicates the original surface finish. Some pits are still present in the C/C surface and the fiber tows that run parallel to the direction of cut on the sample are evident. Scotch™ tape testing showed good adhesion of the IBED titanium coating on all areas of the C/C surface.

It seems, therefore, that the last micron or so of the carbon-carbon surface is weaker than the bulk material. The surface is characterized by dust, and strandlike pieces of carbon fiber.

For this reason, it was decided to reaccomplish these tests, using the same type of carbon-carbon. However, this time the surfaces to be treated were lapped with 5 micron, 1 micron and 0.5 micron lapping compound, to produce a nearly mirrorlike finish. Visual inspection showed that these surfaces were much smoother than the previous batch, and there was less evidence of loose fibers or dusty regions than in the first batch.

**High Thermal Conductivity Composite Fabrication**

The goal for overall thermal conductivity was 500 W/mK at ambient temperature, slightly lower at 900 K.

A preform was prepared by using VGCF fibers heat treated at 2800°C, and furfuryl alcohol as the binder. These preforms were then densified by the chemical vapor infiltration technique at about 1050°C in a gaseous mixture of 80% $CH_4$ and 20% $H_2$. The densification time was varied in order to obtain different final densities. After densification, the specimen was machined to a specimen size suitable for thermal diffusivity measurement.

Optical microscopy analysis was carried to examine the microstructure of both as-

densified and heat treated specimens. The general densification profile across the specimen thickness, the uniformity of densification, the porosity and the morphologies of matrix and fibers were studied.

As noted, the C/C composites consist of VGCF, furfuryl alcohol, and CVI carbon. By the use of polarized light, these three constituents can be distinguished. Highly graphitic VGCF exhibits a cross pattern, and the ungraphitized CVI carbon shows up as purple. Since a limited amounted of binder was incorporated, the binder can only be seen at high magnifications. The binder has a similar color pattern as that of VGCF. Also observable is a certain amount of shrinkage in the binder and fiber, leading to voids between the fiber and binder. The binder is almost as graphitic as the VGCF. However, without any post CVI heat treatment, the matrix carbon shows an isotropic structure.

After the thermal conductivity measurements, the C/C composites were heat treated at 2800°C. The microstructure of these heat treated C/C composites were also examined by optical microscopy. The heat treatment was intended to graphitize the isotropic matrix carbon. However, from the optical analysis, the matrix carbon did not appear to have graphitized remarkably. Other microstructural features are similar to that of as-densified specimens and therefore are not further discussed.

The general trend observed experimentally is that thermal conductivity increases as density or fiber volume increases. The variation of certain data points is believed to be introduced by the fiber-density and matrix-processing variations within the master pieces from which differently processed specimens were obtained.

The second factor relates to the preparation of the VGCF used in the preforms. The degree of graphitization of the fiber possibly affects the graphitization of preform binder, which subsequently affected the graphitization of the matrix carbon. The evidence to support this argument is that, after heat treatment, the specific thermal conductivity of matrix in a composite using heat-treated VGCF in preform fabrication is more than twice of that in a composite with as-grown (un-heat-treated) VGCF in preform fabrication.

Improved understanding of these effects will allow further improvement of thermal conductivity beyond 740 W/mK.

The following assumptions are assumed to control the thermal conductivity during composite fabrication:

a. Matrix contribution to thermal conductivity is negligible prior to heat treatment

b. The increase in specific thermal conductivity due to heat treatment is entirely from the matrix.

One can estimate preform thermal conductivity by the following equation:

$$k_c - k_{n,m}(D_c - D_{pre})$$

where $k_c$ is the conductivity of heat treated C/C, $k_{n,m}$ the specific conductivity of matrix, $D_c$ the density of heat treated C/C, and $D_{pre}$ the density of preform.

Thermal conductivity measurements made before and after graphitization of the densified composites indicated an improvement in specific thermal conductivity by as

much as 38%.

Other research efforts have been directed towards determining the applicability of VGCF fiber for use in metal matrix, carbon matrix, and other composites, characterizing the resulting composites with respect to density, thermal conductivity, thermal expansion, and electrical conductivity. Recent work has also focused on deposition of highly graphitic coatings which exhibit high thermal and electrical conductivity.

**Thermal Conductivity Measurement**

The laser flash diffusivity method for determination of thermal conductivity was used.[2] In this method, the diffusivity, $\alpha$, is measured directly, as well as the specific heat, $C_p$, and the density, $\rho$. The relationship between the thermal conductivity, k, and the directly measured quantities is

$$\alpha = k/\rho C_p$$

The specific heat and density can be accurately measured on small specimens. The diffusivity measurement is obtained by heating the front face of a small specimen with a short (one millisecond or less) burst of radiant energy, usually a laser or xenon flash lamp. The temperature rise on the back face of the specimen is measured by thermocouple or an infrared detector. Diffusivity values can be calculated from the half-time, $t_{1/2}$, required for the back face to reach one-half of its maximum temperature:

$$\alpha = (0.1388\, l^2)/t_{1/2}(2)$$

where l is the thickness of the sample and 0.1388 is the constant corresponding to a rise in temperature of 50 % of the maximum temperature reached.

The temperature range for these measurements was from room temperature to 600°C. Most of the measurements were performed parallel to the fiber direction (X-direction), while some measurements were perpendicular to the fiber direction (Z-direction).

In the microstructural analysis, specimens were mounted in epoxy and then polished. Photos were taken using an optical microscope under polarized light at different magnifications. Both as-densified and heat treated specimens were examined.

Using this method, the thermal conductivity of the VGCF composite was measured to be 740 W/mK, substantially better than the stated goal of 500 W/mK.

**Joining Attempts**

The SAIC carbon-carbon was successfully brazed to titanium by Space Power Inc. These joints were lap joints. Long term creep testing and thermal cycling tests are currently underway to evaluate the effectiveness of the joint so fabricated. Internal thermal stress is a concern for this type of joint.

Attempts were made to diffusion bond SAIC carbon-carbon to titanium pieces. These attempts were only partially successful. While the basic feasibility of the concept

was proven, the butt joints created from this process were not sufficiently strong to overcome the mismatch in thermal expansion coefficient. Hence, the strength of these joints at ambient temperature was very low.

There are two possible reasons for the lower than predicted performance. First, it is possible that the carbon-carbon is substantially weaker near the surface than in the bulk, as described above. This may limit the attainable bond strength using ion beam prepared surfaces. Second, it is possible that the injection of ions into the graphite lattice weakens the lattice by randomizing the atoms.

Use of VGCF composites may be easier than the SAIC or GE carbon-carbons, because the VGCF has a higher thermal expansion coefficients in the plane perpendicular to the direction of highest thermal conductivity.

Additional studies are currently underway to determine whether diffusion bonding to VGCF composites is possible using ion-beam treated surfaces. At present, this answer is not known.

In summary, the experimental program had some notable successes, such as the production of a VGCF composite with thermal conductivity of 740 W/mK, well above the goal of 500 W/mK.

Yet unexpected problems were encountered in the ion beam deposition of titanium to carbon-carbon. It is believed that the near-surface region of carbon-carbon is substantially weaker than the bulk. Most of the effort in this project was expended on solving this problem. At this writing, the resolution of this issue has been only partially successful, and the applicability of the ion-beam method to carbon-carbon is still in doubt.

## V. Radiator Analysis

The illustration below depicts a radiator/fin geometry designed for minimum mass. The interaction zone at the joint is considered to have an effective thickness of Figure 1 illustrates a possible fin/heat pipe interface. The interaction zone at the joint is considered to have an effective thickness of $\Delta L$, which is obviously in the y direction. The fin has a thickness t in the z direction. The length of the heat pipe is arbitrary. A differential energy balance yields the following equation for the temperature distribution:

$$\frac{d^2T}{dy^2} - \frac{\sigma \varepsilon \Delta T^4}{kH}$$

subject to the boundary conditions

$$\frac{dT(y = 0)}{dy} = 0 \text{ and } T(y_o) = T_e$$

This equation is solved by

$$B(0.3,0.5) - B_{T^*}(0.3,0.5) = y_o\left(\frac{20\sigma T_{min}}{k\delta_o}\right) ,$$

where B represents the Beta function and By represents the incomplete Beta function, and T* is nondimensional temperature $(T_e/T)^5$.

The heat dissipated by the fin is equal to

$$q = -kL\delta \left.\frac{dT}{dy}\right|_{y=y_o}$$

Optimization of the radiator weight is a function of several nonlinear variables. The radiator weight is a nonlinear function of the heat load it must carry; plus the reliability requirement against micro-meteoroid penetration; the fin material density; thermal conductivity; area and volume constraints; etc.

The fin efficiency, defined as the actual amount of heat rejected divided by the theoretical limit, is equal to

$$\eta = \frac{2k\delta_o \left(\frac{\sigma\varepsilon}{5k\delta_o}\right)^{1/2} \left(T_o^5 - T_e^5\right)}{2\sigma y_o \varepsilon T_o^4}$$

For the sake of simple analysis, it is assumed that the heat pipe is a line heat source at a constant temperature of 900 degrees. The fin is assumed to be a constant-thickness VGCF composite with thermal conductivity 500 W/mK at 900 K, density of 2.0 g/cm3 and a graybody emissivity of 0.90. A parametric analysis was performed to determine the approximate maximum heat rejection per unit area as a function of total heat load, as well as the total fin length required.

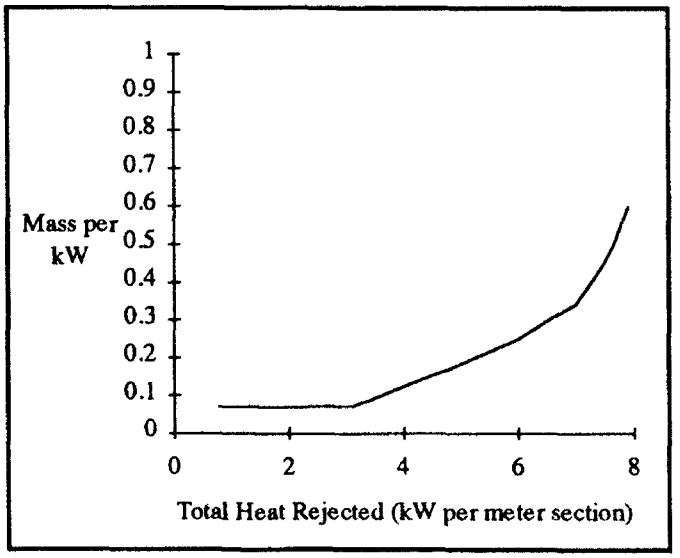


Figure 4. Specific Mass vs. Total Thermal Load per Unit Length of Heat Pipe

Use of lightweight fins will result in a mass reduction at the expense of an increase in area. At higher heat loads, the fins must be made longer and thicker until there is no benefit in mass at all. Assuming a heat pipe radiator specific power will fall in the range of 0.4 kg/kW at 900 K, this means that a crossover point is around 6-7 kW per meter of length of heat pipe, for the case of perfect thermal contact between heat pipe and fin. At this point there can be no mass benefit for using fins.

As can be seen in Table III.a and III.b, the picture changes significantly if it is assumed that a braze joint with a small interaction zone (say, 2 mm with a thermal conductivity of 20 W/mK) exists.

The effectiveness of the fin is substantially reduced in this case.

**Table III.a Parameters for Carbon Fins Only**

| | | |
|---|---|---|
| Thermal Conductivity | W/mK | 500 |
| Fin Length | cm | 17 |
| Fin Thickness | cm | 0.1 |
| $T_{base}$ | K | 900 |
| $T_{end}$ | K | 530 |
| Thermal Power, 1 m section | kW | 3.35 |
| Axial Heat Flux | $W/cm^2$ | 335 |
| Efficiency | % | 58 |
| Specific Mass | kg/kW | 0.103 |

**Table III.b. (Pessimistic) Fin/Braze Joint Performance**

| | | |
|---|---|---|
| Joint Thermal Conductivity | W/mK | 20 |
| Joint Thickness | cm | 0.2 |
| $T_o$ | K | 900 |
| $T_{base}$ | K | 712 |
| Thermal Conductivity | W/mK | 500 |
| Fin Length | cm | 17 |
| Fin Thickness | cm | 0.1 |
| $T_{end}$ | K | 530 |
| Thermal Power, 1 m section | kW | 1.87 |
| Efficiency | % | 32 |
| Specific Mass | kg/kW | .262 |

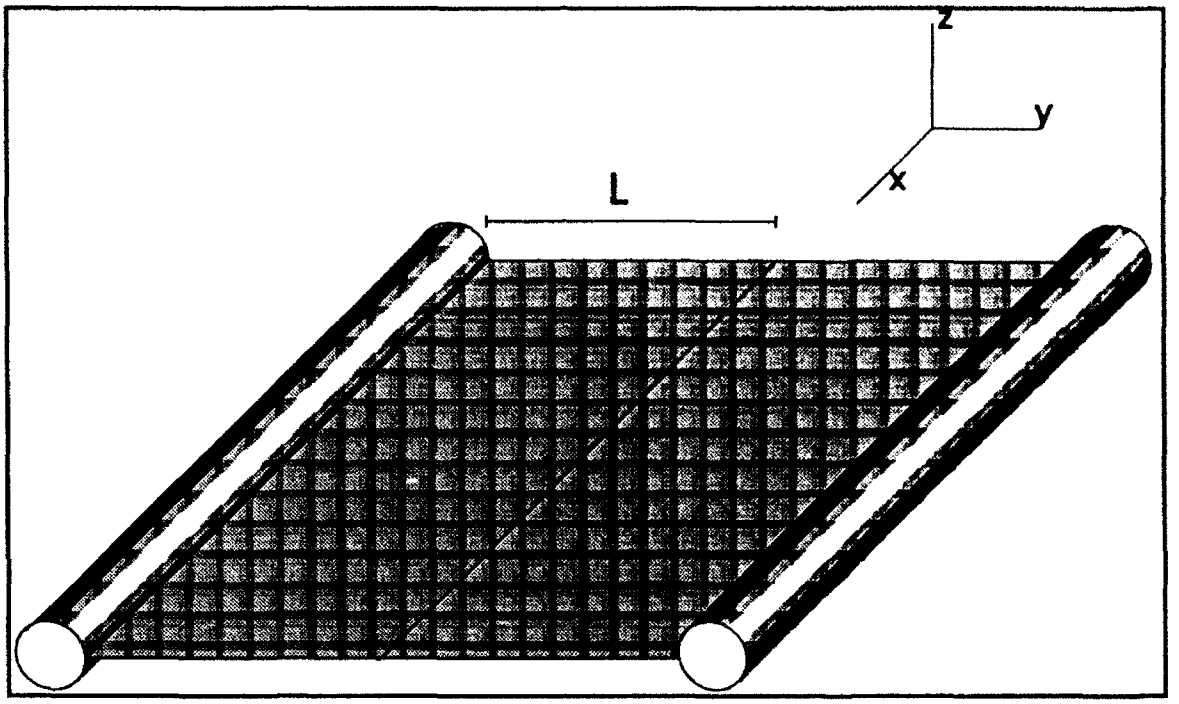


Figure 5. Radiator Layout

In the general case the quantity of heat Q through the joint with area S during the period of time $\tau$ is described by the following equation:

$$q = kS \frac{\Delta T}{\Delta L} \tau$$

where k is the thermal conductivity, $\Delta L$ is the thickness of the joint, and $\Delta T$ is the temperature drop through the joint.

From the point of view of high thermal conductance we must create the joint with minimum possible thickness $\Delta L$ and use joint materials with high k.

Thus, the most favorable case is to perform direct diffusion bonding between carbon-carbon and titanium. In this case $\Delta L$ is about a micron or less.

Strangely, the formation of titanium carbide in the joint could actually improve the thermal conductivity, since the thermal conductivity of titanium carbide is higher than that of pure titanium. It is recognized that the chemical bonds formed by titanium ion beam injection are certain to be much different than those of titanium carbide. Nonetheless, should the stable titanium carbide form, it is likely that it could result in increased brittleness.

To prevent carburizing of titanium, it is possible to metallize the joining surface with nickel. As noted above, this may not be necessary, owing to the high thermal conductivity of TiC and the non-equilibrium nature of the chemical bonds formed between high energy titanium ions and the host lattice.

Another alternative is to use a copper interlayer. However, copper forms a brittle intermetallic phase with titanium. To obviate these negative factors, it is possible to use

niobium, molybdenum or vanadium interlayers between the copper and titanium. Thin coatings of niobium, molybdenum or vanadium can be formed on titanium or copper before diffusion bonding.

For bonding the copper interlayer to the titanium-implanted carbon material, it is possible to use contact melting. The melting point of the eutectic $Ti_2$-$Cu_3$-$TiCu_3$ is 870 °C. This temperature satisfies the technological conditions of diffusion bonding. A thin Ti layer on carbon material reacts with copper and completely melts. In the case of excess copper, we may consider forming the melt as an alloy enriched with copper. Increasing the temperature to 1000 °C, we may decrease the Ti concentration in copper. After finishing the process, a solid solution of Ti in Cu will result.

The solubility of Ti in Cu is rather low (less than 1%) and it does not affect the thermal conductivity of copper. On the other hand, the presence of titanium in copper melt improves the wetting of carbon with copper melt. For improving the thermal characteristics of joints between copper and refractory metals, it is sometimes recommended to use titanium or nickel interlayers. Thus the structure of one of the variants for bonding is shown below.

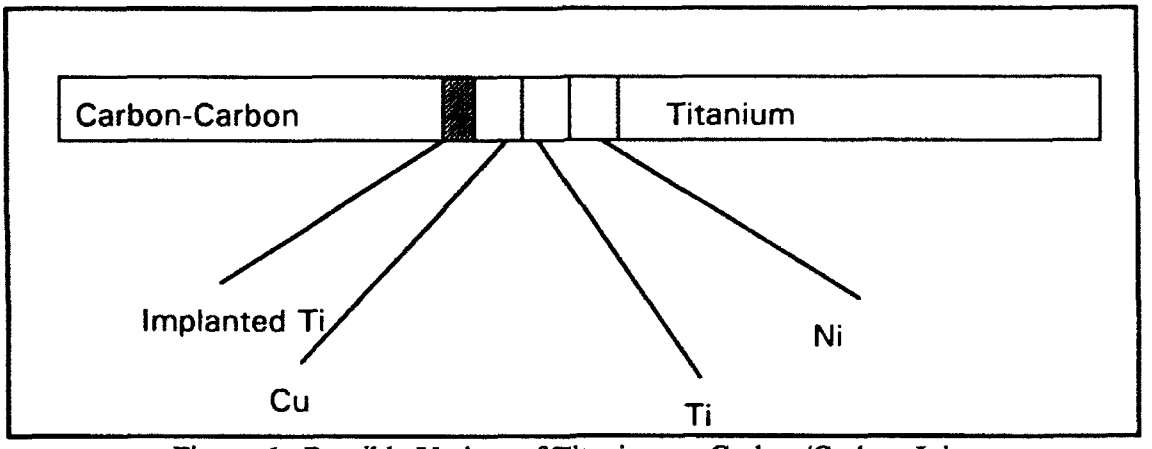


Figure 6. Possible Variant of Titanium to Carbon/Carbon Joint

## VI. Recommendations

The present effort was successful in that it demonstrated the technical feasibility of the IBED method to alter the surfaces to be joined. It can be inferred that the thermal conductance through the joint is much higher than can be achieved through other means. However, we did not show that superior strength was attained through this process, and the case has not yet been made that this is indeed the preferred method for making bonds between carbon carbon and titanium.

It further became obvious as the program proceeded that the carbon-carbon was more challenging than initially believed. We had counted on the enormous strength of the ion-beam deposited bonds to overcome substantial thermal expansion mismatches. This was not the case, as the metal and composite delaminated at the interface. We believe that this was due to poor structural integrity of carbon-carbon at the surface of the material, due to microscopic damage and weakening caused during cutting the material with a

diamond saw.

To obviate this problem, we should use thicker depositions of titanium, which will completely fill in any pores which might exist, and to add structural strength to any loose fibers or weak areas on the surface of the composite. Titanium deposition could be accomplished by an IBED technique followed by sputtering or vapor deposition technique.

It is also possible to correct for the thermal expansion coefficient mismatch by using a layered approach. However, this leads to a higher thermal resistance between the composite fin and the metal tube, which was one of the things we were trying to avoid.

A better approach would be to heat the substrate to operating temperature during deposition, so that the minimum internal stress point will occur at operating temperature. This will require modifying the vacuum deposition apparatus.

Inherently, there is no reason to believe that this method would not work for very high temperature applications if refractory metal is substituted for titanium. In this case, joints could be made up to 3000 K. We are also interested in considering other types of joints such as ceramic to metal and ceramic to ceramic joints.

**References.**


1. C. A. Vansant and W. C. Phelps, Jr., "Carbide Formation from Beta-Titanium and Graphite, *Transactions of the American Society for Metals*, Vol. 59, 1966 pp. 105-112.

2. G. E. Hollox, "Microstructure and Mechanical Behavior of Carbides," *Materials Science and Engineering*, Vol. 3, 1968/69, pp. 121-137.

3. Dillon, R.O., Ahmed, A., Woollam, J., Lake, M.L., "High Temperature Resistivity of Carbon Fibers", Bull. Am. Phys. Soc., 33 #3, 1988.

4. Brito, K.K., Hagerhorst, J., Lake, M.L., "Electrical Resistivity of Vapor Grown Carbon Fibers," Bull. Am. Phys. Soc., 33 #3, 1988.

5. Lake, M.L., Woollam, J., et al, "High Temperature, Electrically Conductive Graphitic Composites," Proceedings of the SPIE, 871 Space Structures, Power and Power Conditioning (1988) pp. 89-95.

6. Lake, M.L., Dillon, R.O., Hickok, J.K., Brito, K.K., and Woollam, J., "High Temperature Lightweight Composites for Space Nuclear Power," Final Report, Contract #F33615-87-C-2833, June, 1988.

7. Lake, M.L., "Fabrication and Characterization of Boronated Carbon Fibers and Electrical Conductors" Argonne National Laboratory Contract #7202401, December 1987.

8. Lake, M.L., Brito, K.K., Hickok, J.K., "Novel Materials for Electromagnetic Railguns" Final Report, Contract #F33615-88-C-2805, December, 1988.

9. Lake, M.L., Lin, R.Y., Hickok, J.K., and Brito, K.K., "Oxidation Properties of Vapor Grown Graphite Fibers" Final Report, NSF Grant #ISI-8760421, October, 1988.

10. Lake, M.L., Woollam, J.A., and Ahmed, A., "Growth of Boron Doped Carbon Fibers" Final Report, ANL Contract #60762401, November, 1986.

11. Ahmed, A., Rost, M., Meyer, D., Dillon, R., Woollam, J., and Lake, M.L., "Electrical Resistivity (4oK to 2100oK) of Annealed Vapor Grown Carbon Fibers" Applied Physics Communications, June, 1987.

12. Brito, K.K., Anderson, D.P., Rice, B.P., "Graphitization of Vapor Grown Carbon Fibers", 34th International SAMPE Conference, Reno, NV, May 1989.

13. Hickok, J.K., Lide, A.M., Lake, M.L., "CVD/Hybrid Fibers for Structural, Thermal, and Electrical Applications," Final Report, Contract #N60921-89-C-0175, December, 1989.

14. Lake, M.L., Hickok, J.K., Brito, K.K., Begg, L.L., "Vapor Grown Carbon Fiber for Space Thermal Management Systems", to be presented at the 35th International SAMPE Symposium and Exhibition, April 2-5, 1990.

15. A. H. Deutchman and R. J. Partyka, "Wear Resistant Performance of Ion Implanted Alloy Steels," Proceedings of the NATO Advanced Study Institute: Surface Engineering, Les Arcs, France, July 1983, R. Kossowsky, ed.

16. R. J. Partyka and A. H. Deutchman, "A Prototype Ion Implanter for Industrial Tool and Die Processing," Proceedings of the NATO Advanced Study Institute: Surface Engineering, Les Arcs, France, July 1983, R. Kossowsky, ed.

17. A. H. Deutchman and R. J. Partyka, "Ion Implantation: A New Surface Treatment Technology for Stamping Tooling," Proceedings-High Speed Stamping and Dies, Society of Manufacturing Engineers, Louisville, Kentucky, November 1985, p. 96.

18. R. J. Partyka and A. H. Deutchman, "Ion Implantation: A New Surface Treatment Technology for Can Manufacturing Tooling," Proceedings - Effective Can Manufacturing Technology, Society of Manufacturing Engineers, Schaumberg, Ill, September 10-12, 1986.

19. A. H. Deutchman and R. J. Partyka, "Ion Implantation: A New Surface Treatment Technology for the Manufacture of Orthopaedic Implants," Proceedings - Effective and Emerging Implant Manufacturing and Material Technology, Society of Manufacturing Engineers, Itasca, Ill, Dec 2-4, 1986.

20. A. H. Deutchman and R. J. Partyka, "Practical Applications of Ion Beam Mixing: A

New Surface Treatment Technique," Industrial Heating, Vol. LV, No. 2, 1988.

21. M. M. Lemcoe, A. H. Deutchman et al., "Bonding Gauges to Carbon/Carbon Composites," NASA Tech Briefs, Vol 13, No. 9, Sept 1989, p. 102.

22. R.E Taylor, Thermophysical Properties Research Laboratory Report 181A, July, 1985.

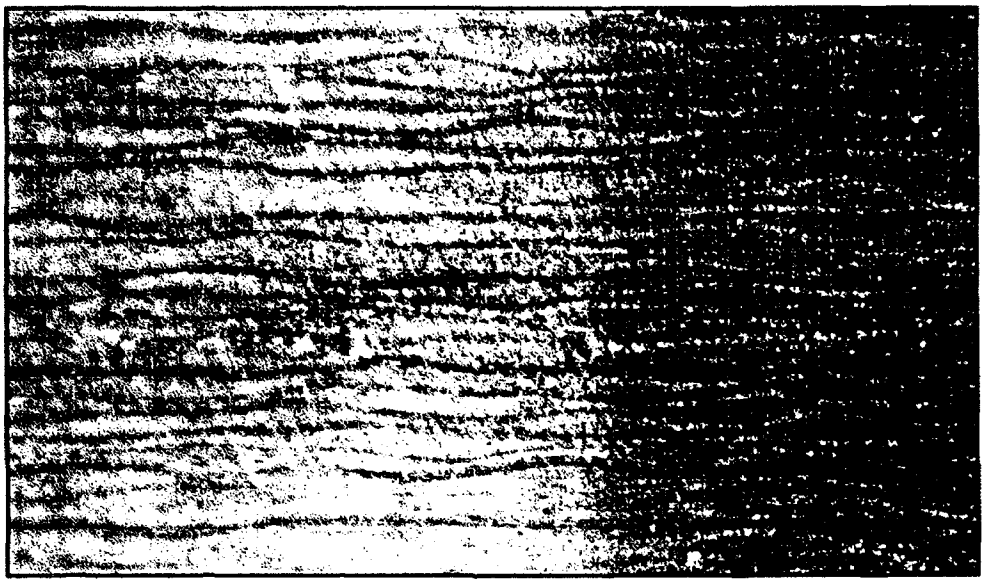

Figure A-1. Batch 1 Sample (0.5 micron Ti)

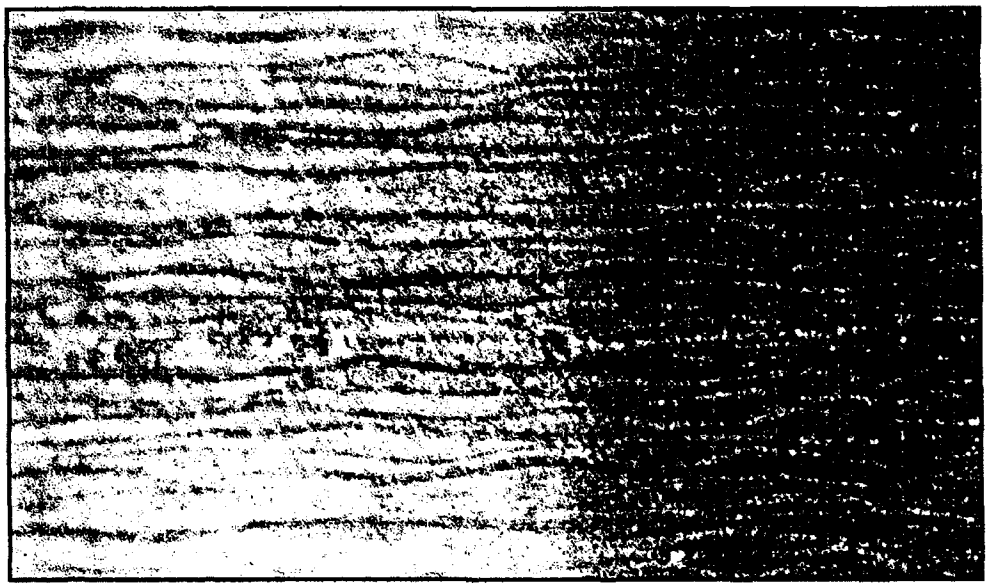

Figure A-2. Batch 1 Sample (0.5 micron Ti)

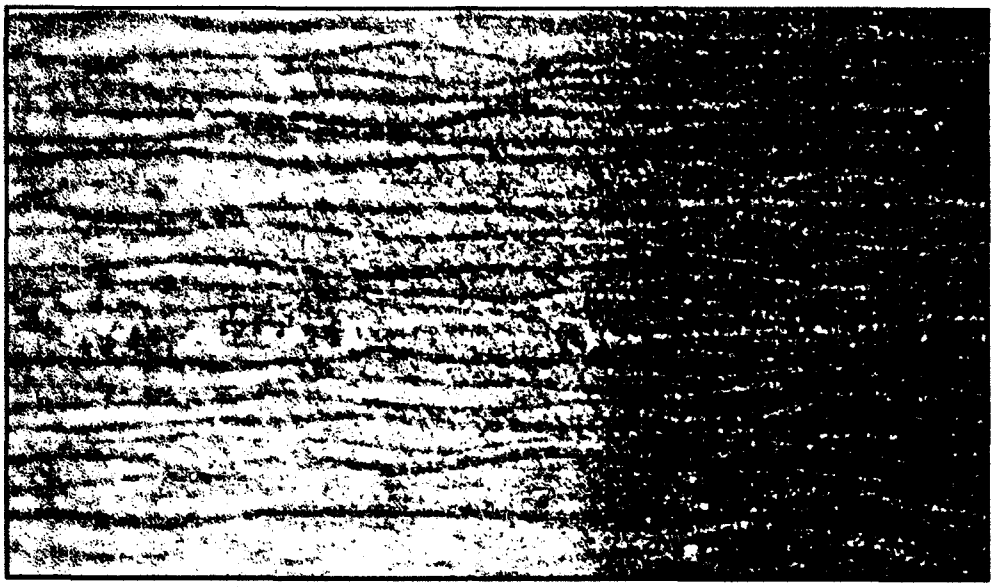

Figure A-3 Batch 1 Sample (0.5 micron Ti)

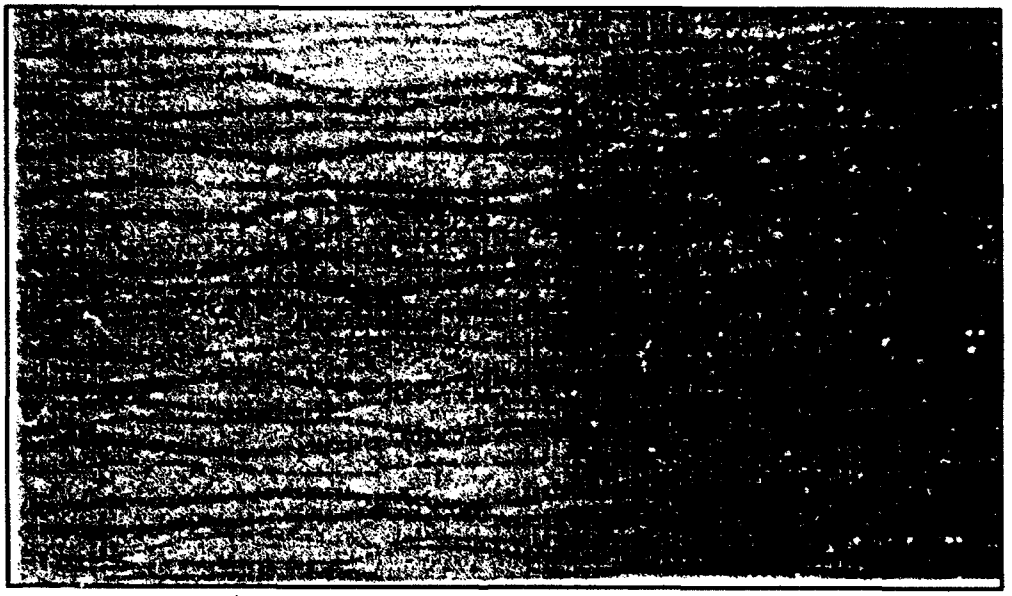

Figure A-4. Batch 2 Sample (0.5 micron Ti)

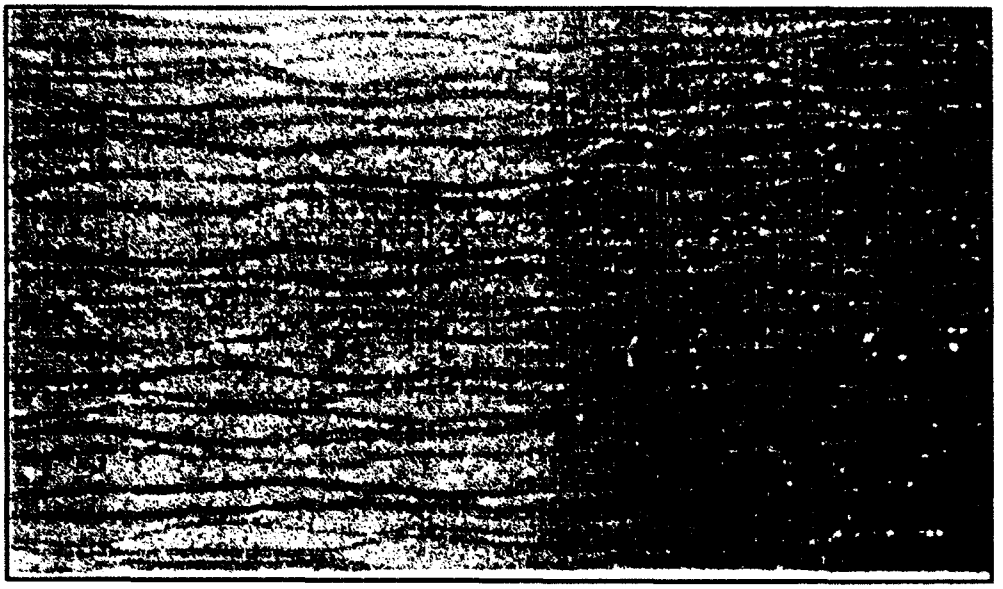

Figure A-5. Batch 2 Sample (0.5 micron Ti)

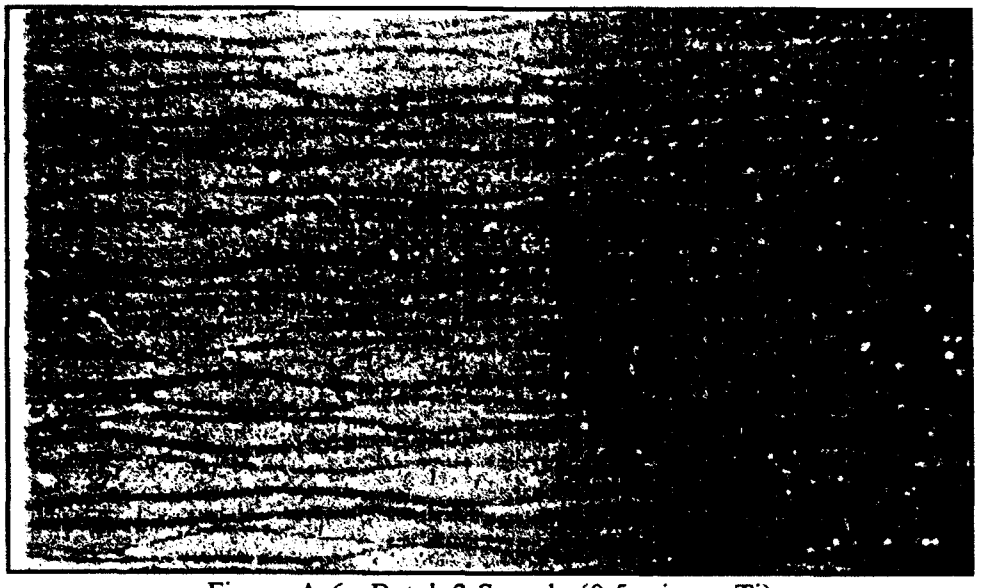

Figure A-6. Batch 2 Sample (0.5 micron Ti)

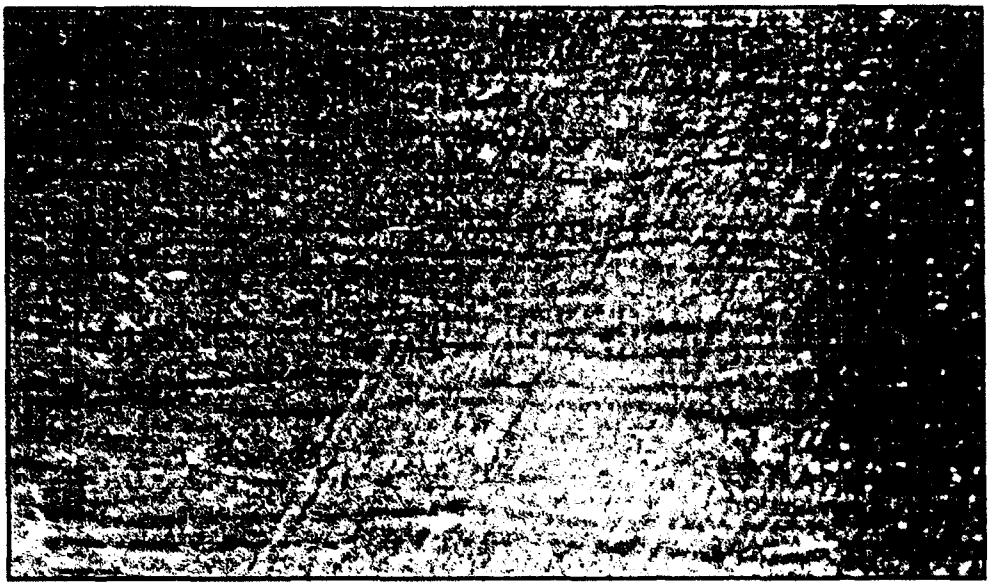

Figure A-7. Batch 3 Sample (0.5 micron Ti)

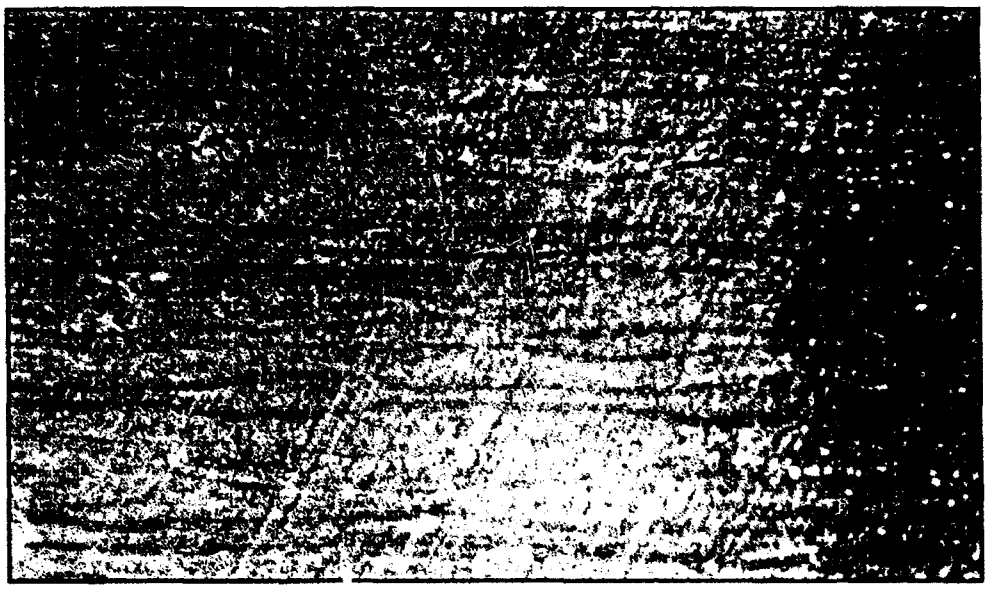

Figure A-8. Batch 3 Sample (0.5 micron Ti)

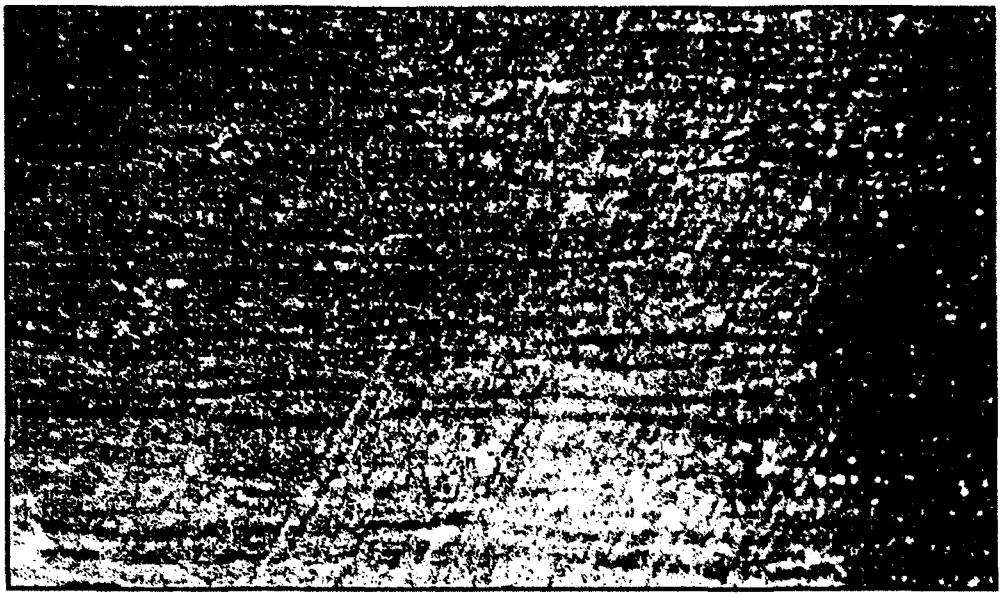

Figure A-8. Batch 3 Sample (0.5 micron Ti)

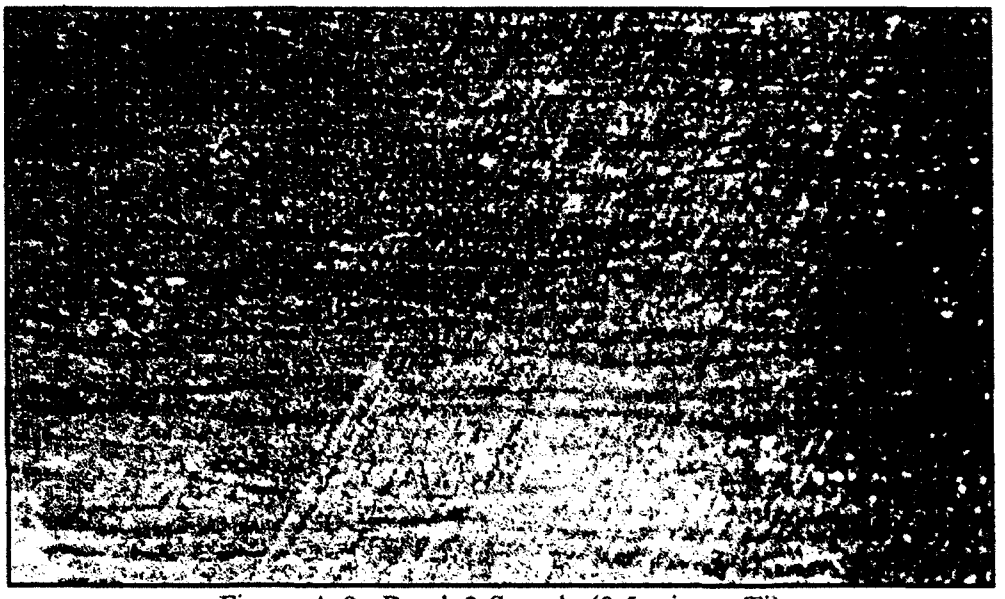

Figure A-9. Batch 3 Sample (0.5 micron Ti)

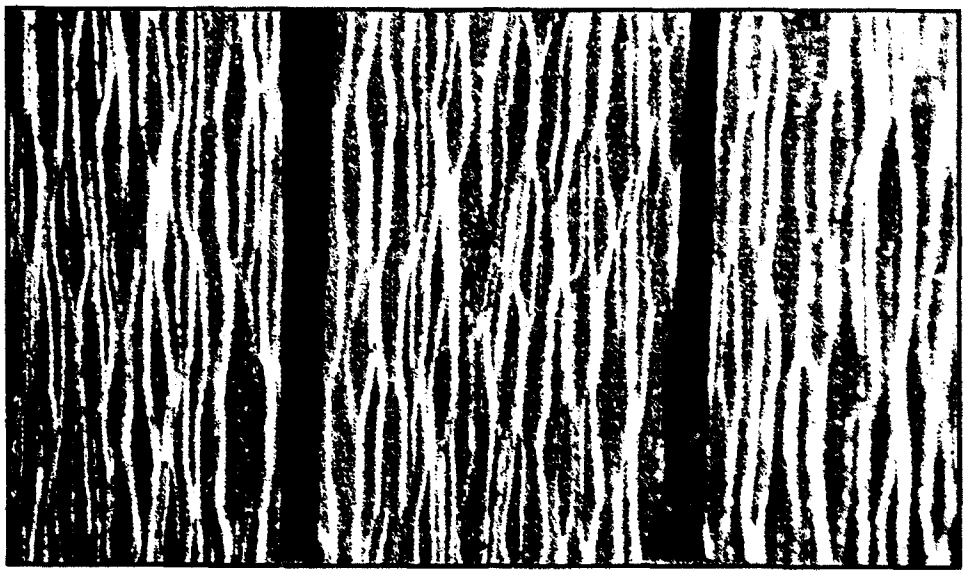

Figure A-10. Batch 3 Sample (0.5 micron Ti)

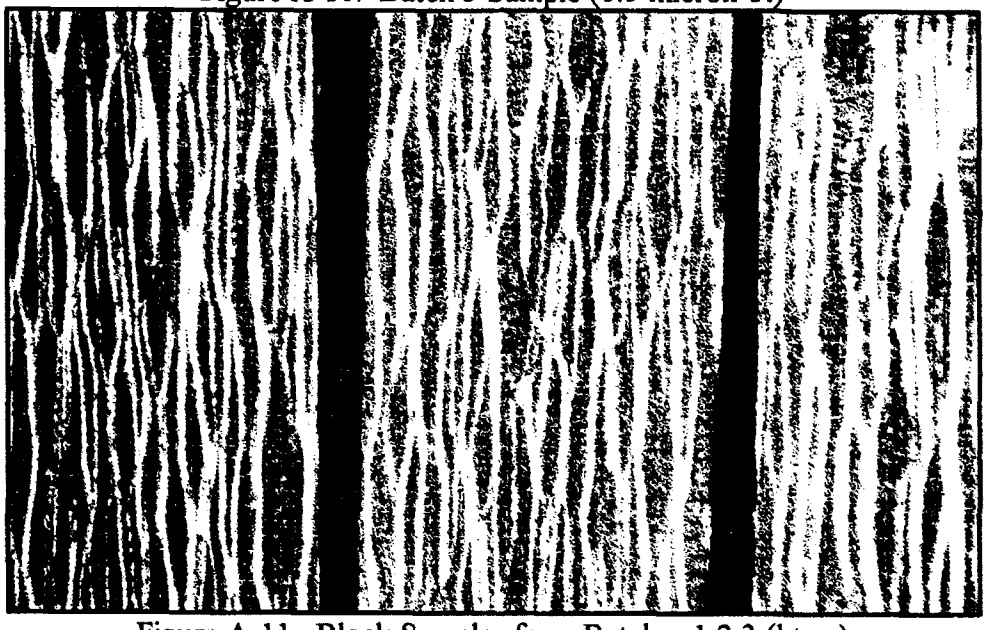

Figure A-11. Block Samples from Batches 1,2,3 (l to r)

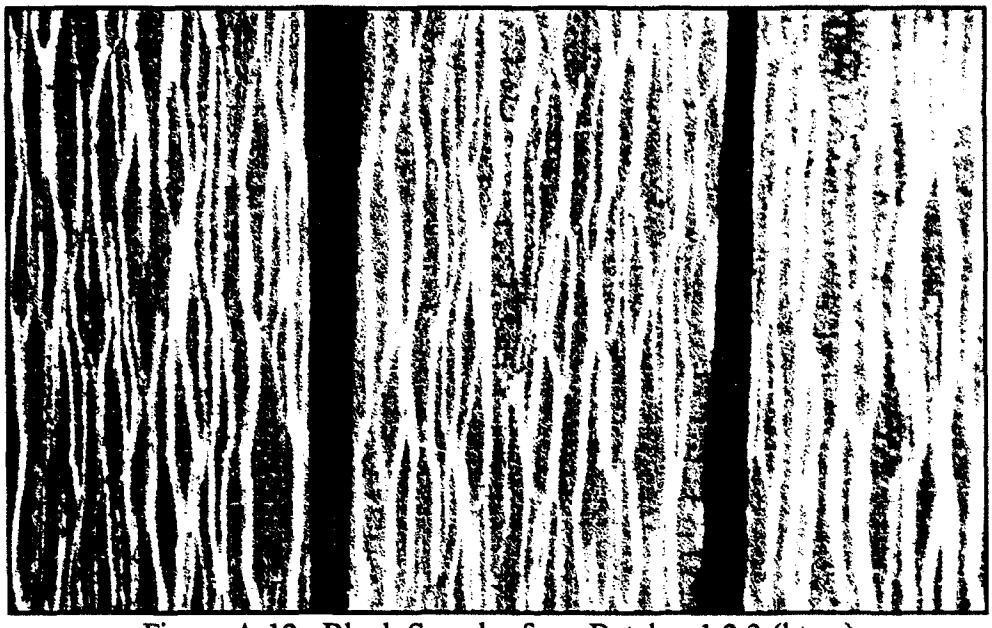

Figure A-12. Block Samples from Batches 1,2,3 (l to r)

Figure A-13 Batch 4 Sample, Uncoated

Figure A-15. Batch 4 Fin Sample (Uncoated)

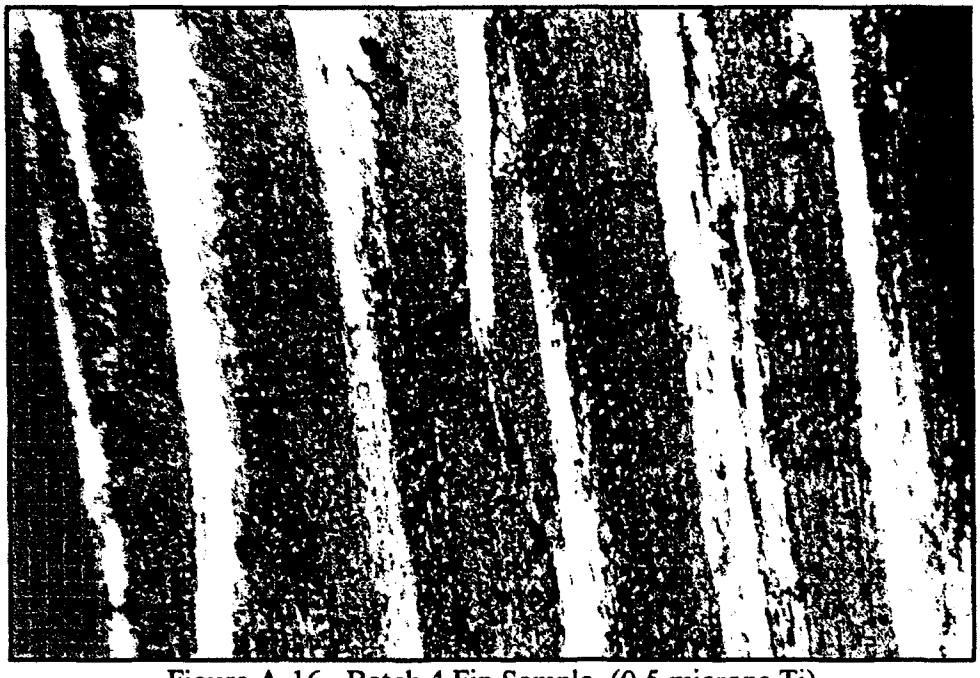

Figure A-16. Batch 4 Fin Sample, (0.5 microns Ti)

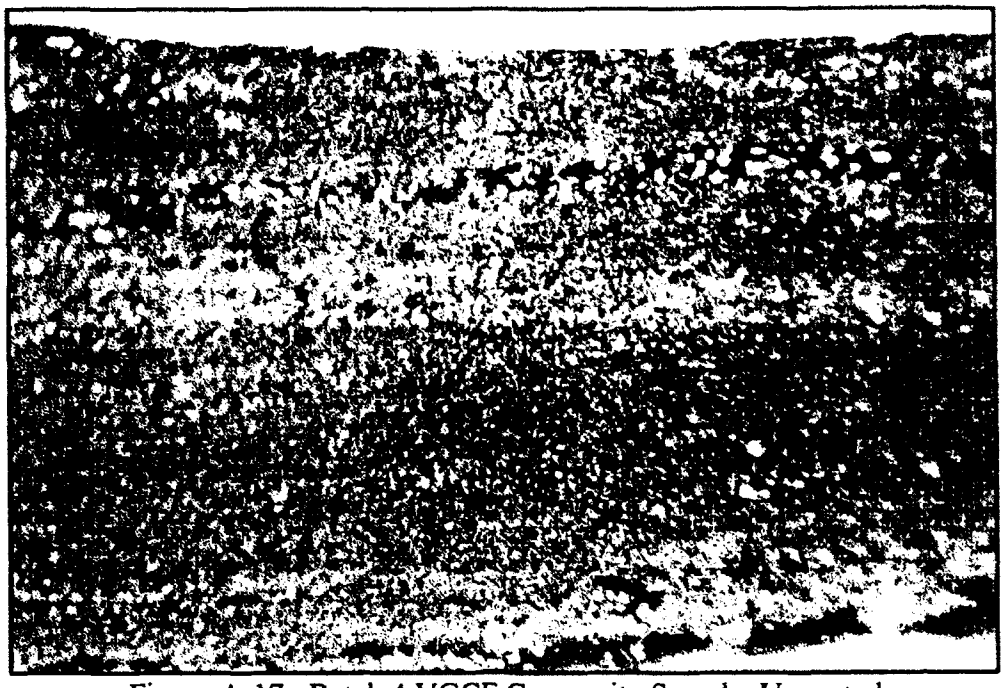

Figure A-17. Batch 4 VGCF Composite Sample, Uncoated

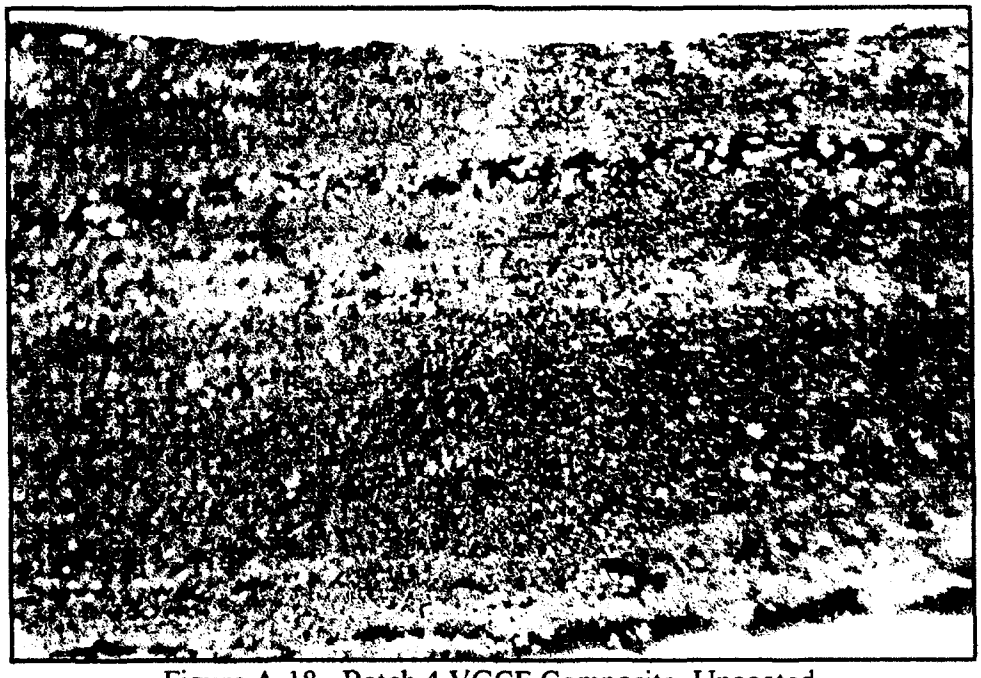

Figure A-18. Batch 4 VGCF Composite, Uncoated.

Figure A-19. Batch 4 VGCF Composite, Coated

Figure A-20. Batch 4 VGCF Composite, Coated

Figure A-21. Batch 4 VGCF Composite, Coated

Figure A-22. GE Material, Polished, (3.0 micron Ti)

Figure A-23. GE Material, Polished, (3.0 micron Ti)

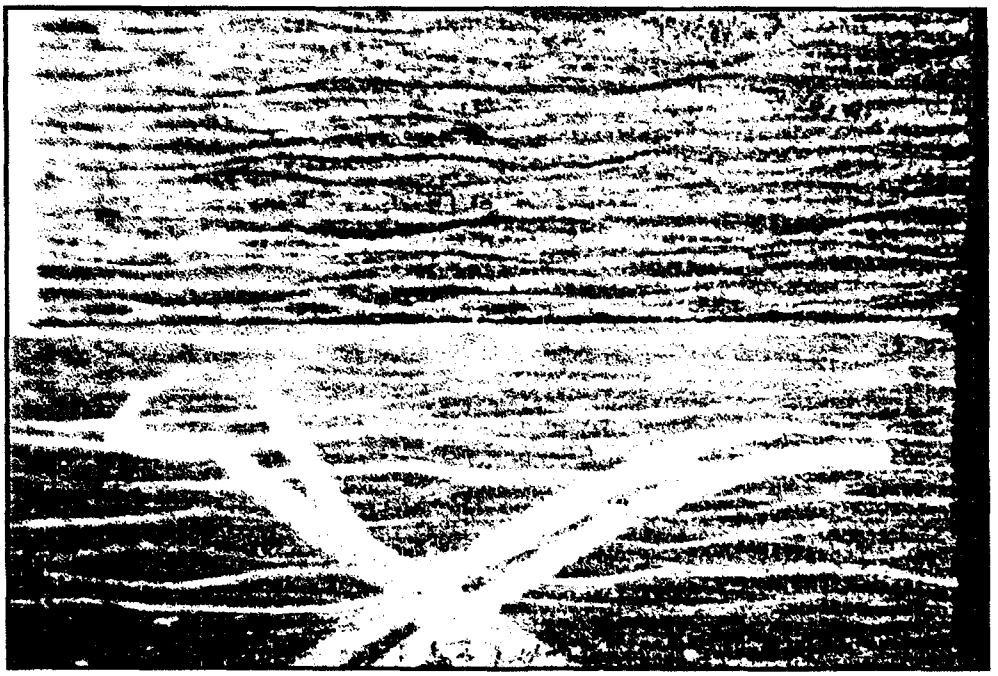

Figure A-24. GE Material, Polished vs. Unpolished, 12x Mag.

Figure A-25. GE Carbon/Carbon, Polished vs. Unpolished, 12x

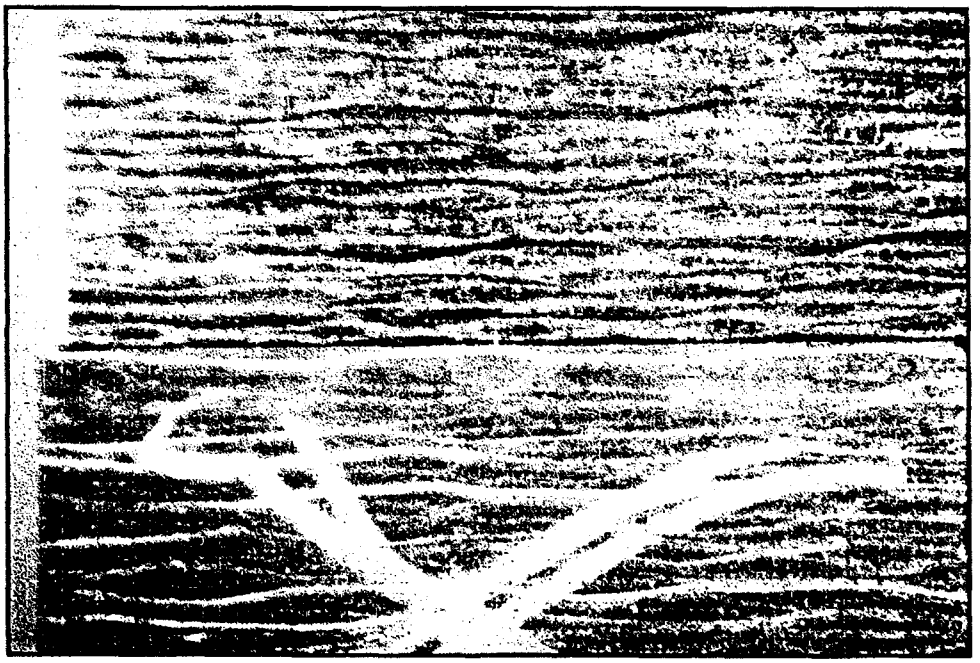

Figure A-26 GE Carbon/Carbon, Polished vs. Unpolished, 12x

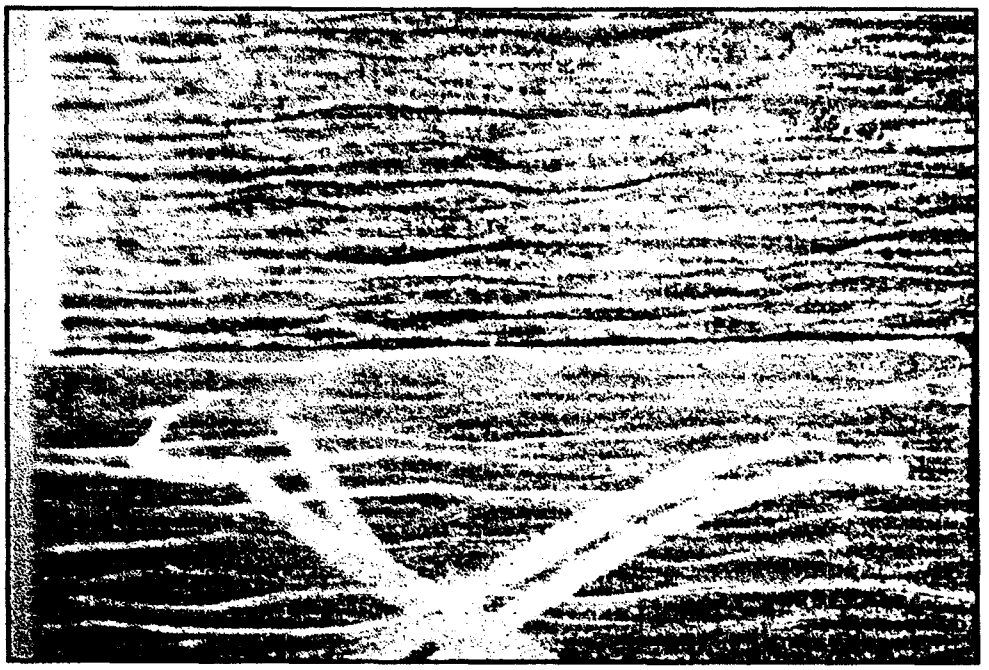

Figure A-27. GE Carbon/Carbon, Polished vs. Unpolished, 12x

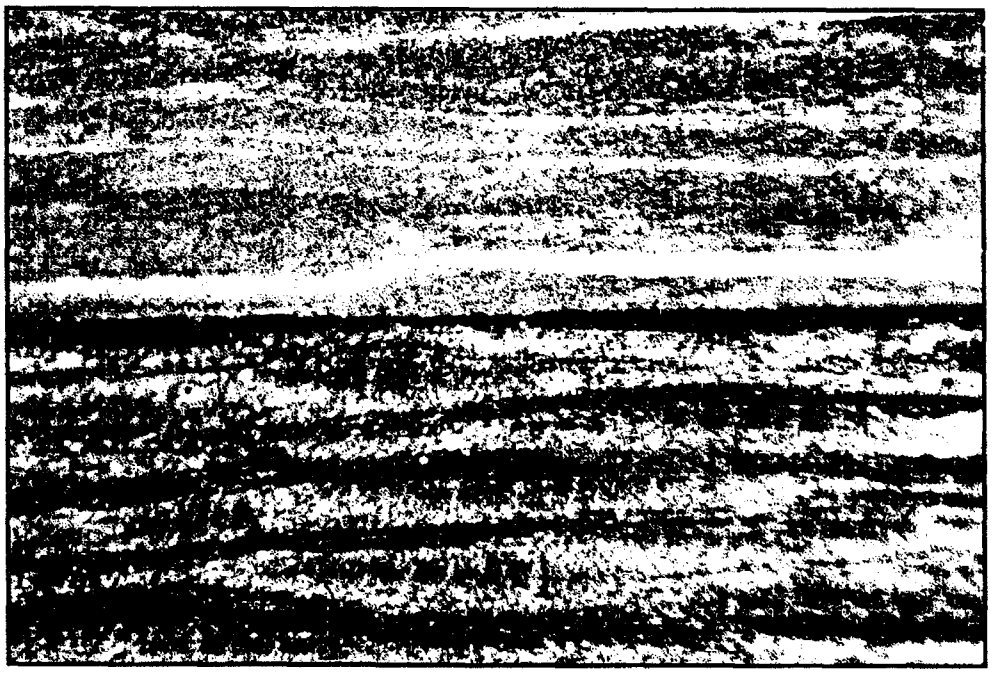

Figure A-28. GE Carbon/Carbon, Polished vs. Unpolished, 35x

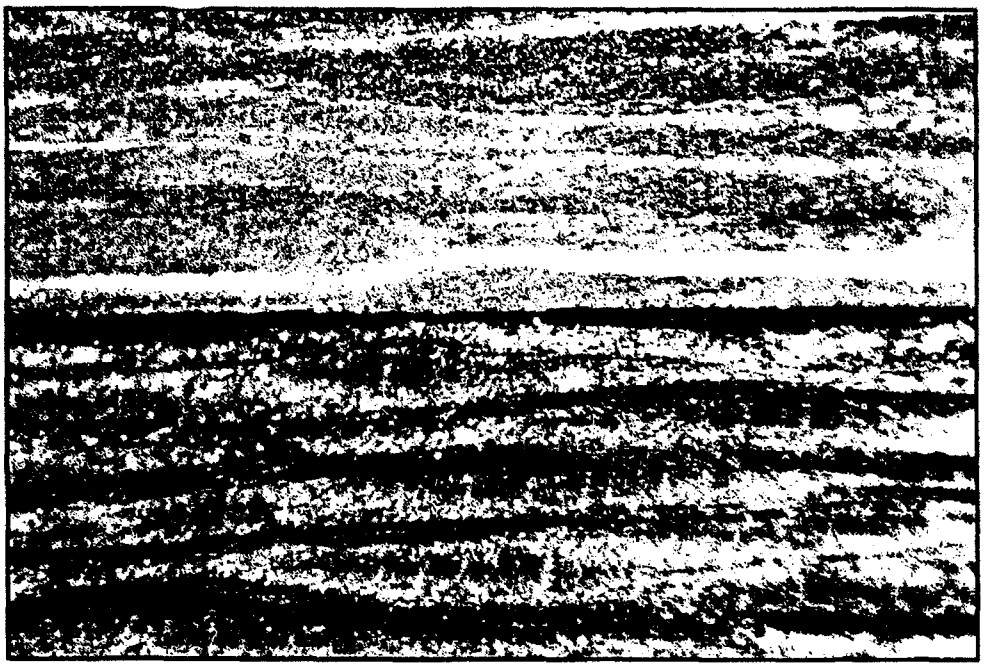

Figure A-29. GE Carbon/Carbon, Polished vs. Unpolished, 35x

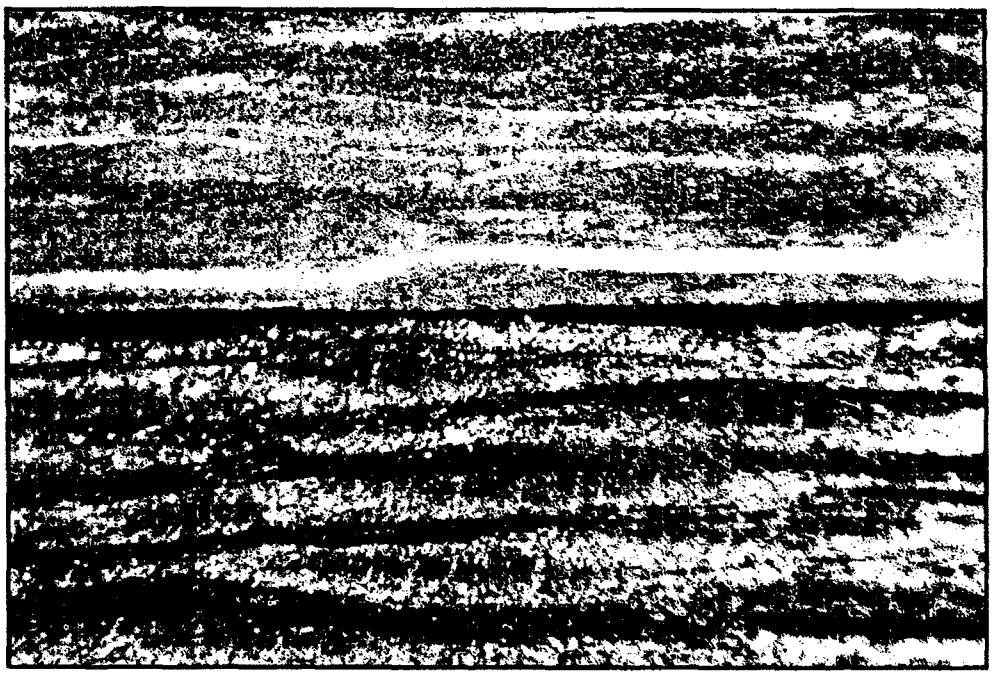

Figure A-30. GE Carbon/Carbon, Polished vs. Unpolished, 35x

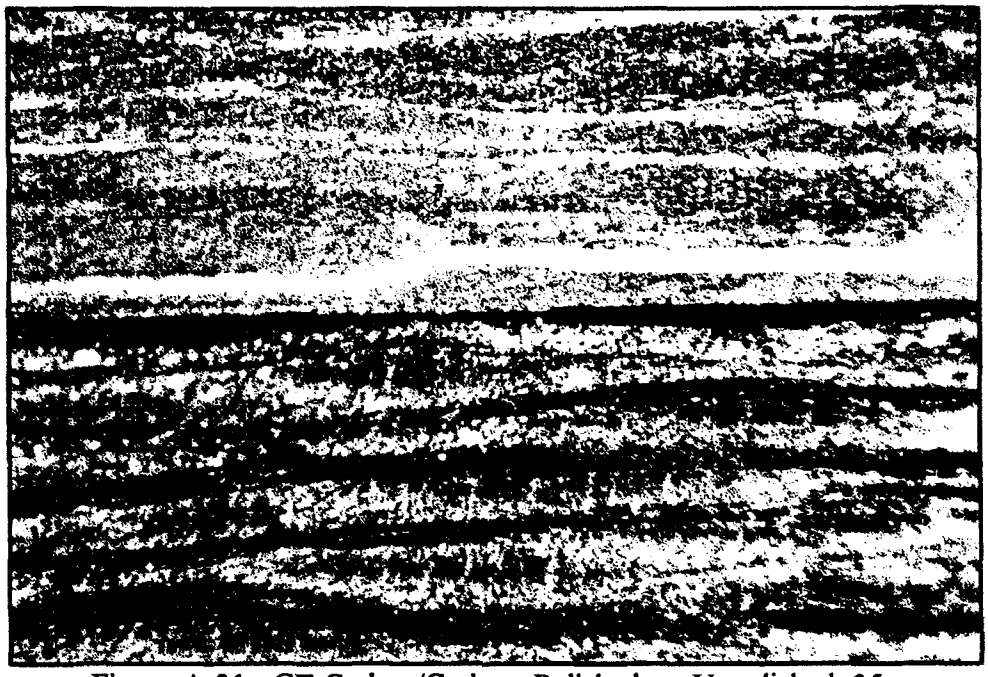

Figure A-31. GE Carbon/Carbon, Polished vs. Unpolished, 35x

Figure A-32. SAIC Carbon/Carbon, Polished vs. Unpolished, 12x

Figure A-33. SAIC Carbon/Carbon, Polished vs. Unpolished, 12x

Figure A-35. SAIC Carbon/Carbon, Polished vs. Unpolished, 12x

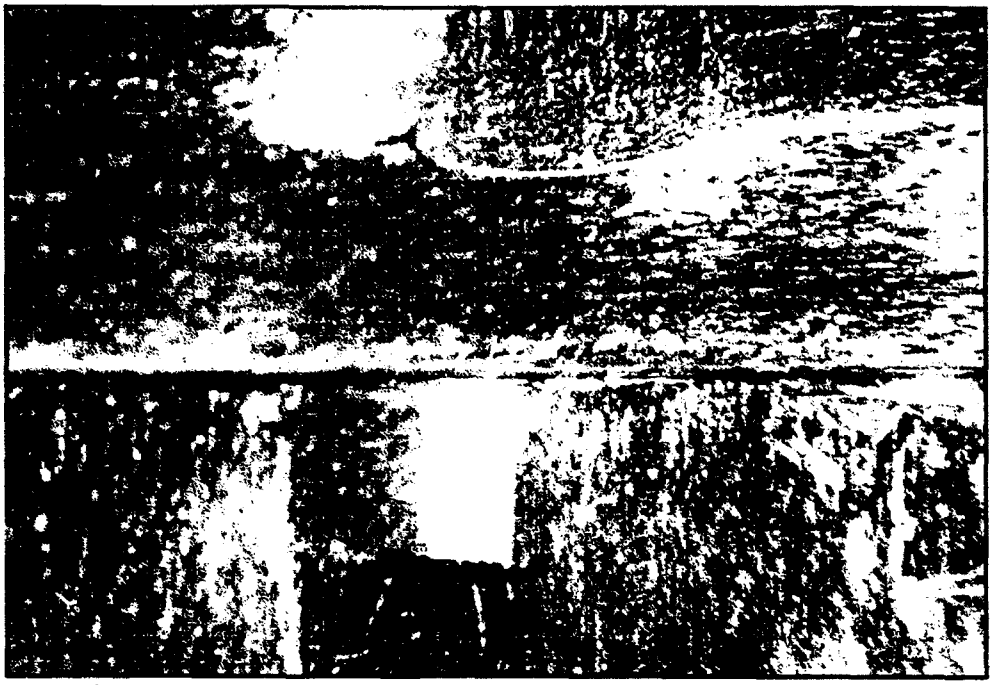

Figure A-36. SAIC Carbon/Carbon, Polished vs. Unpolished, 35x

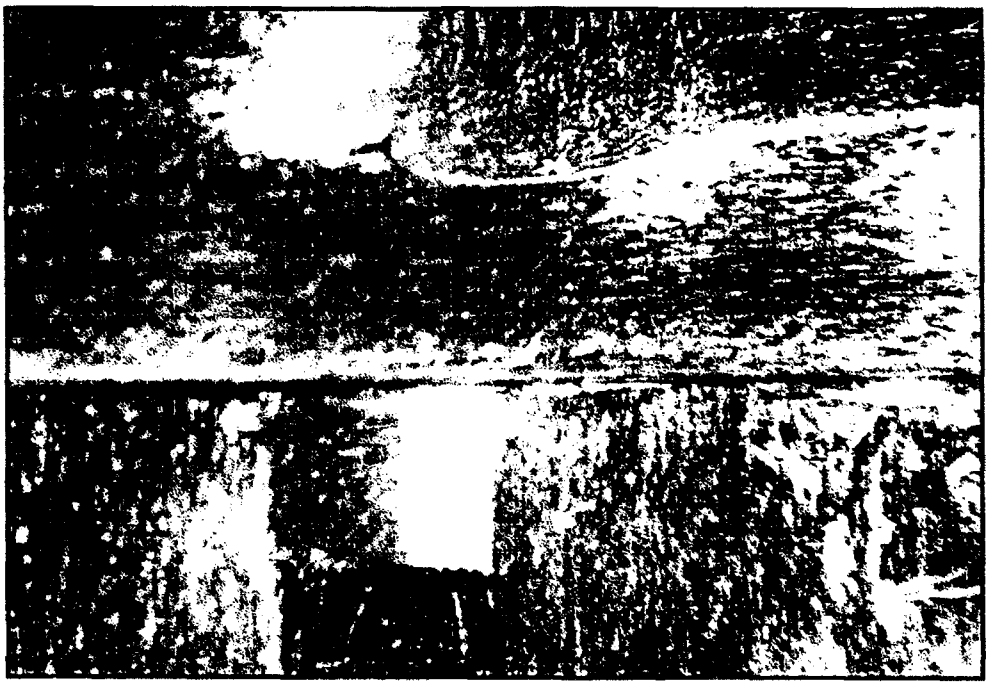

Figure A-37. SAIC Carbon/Carbon, Polished vs. Unpolished, 35x

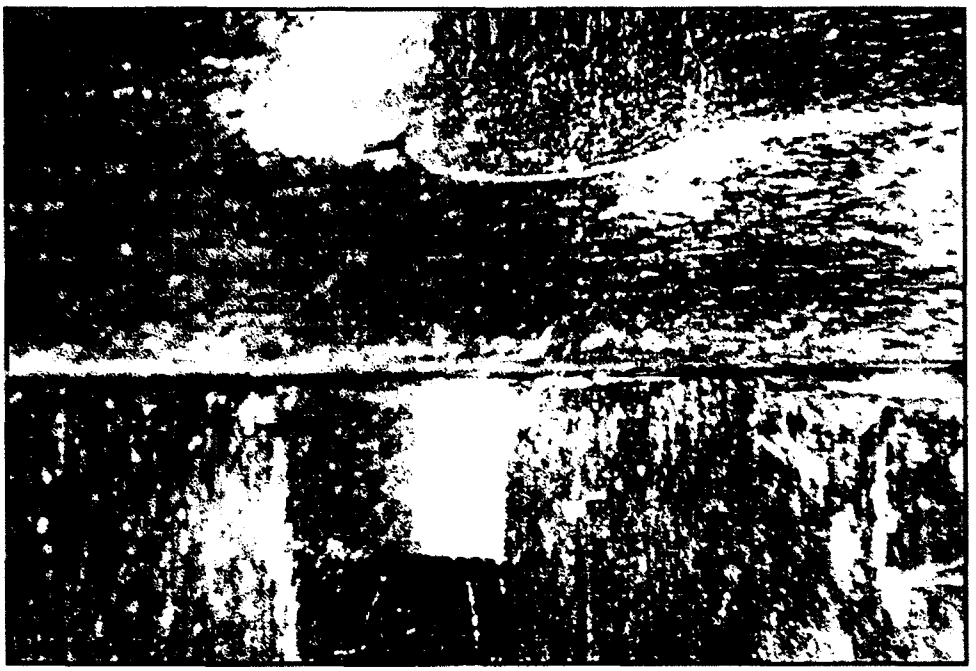

Figure A-38. SAIC Carbon/Carbon, Polished vs. Unpolished, 35x

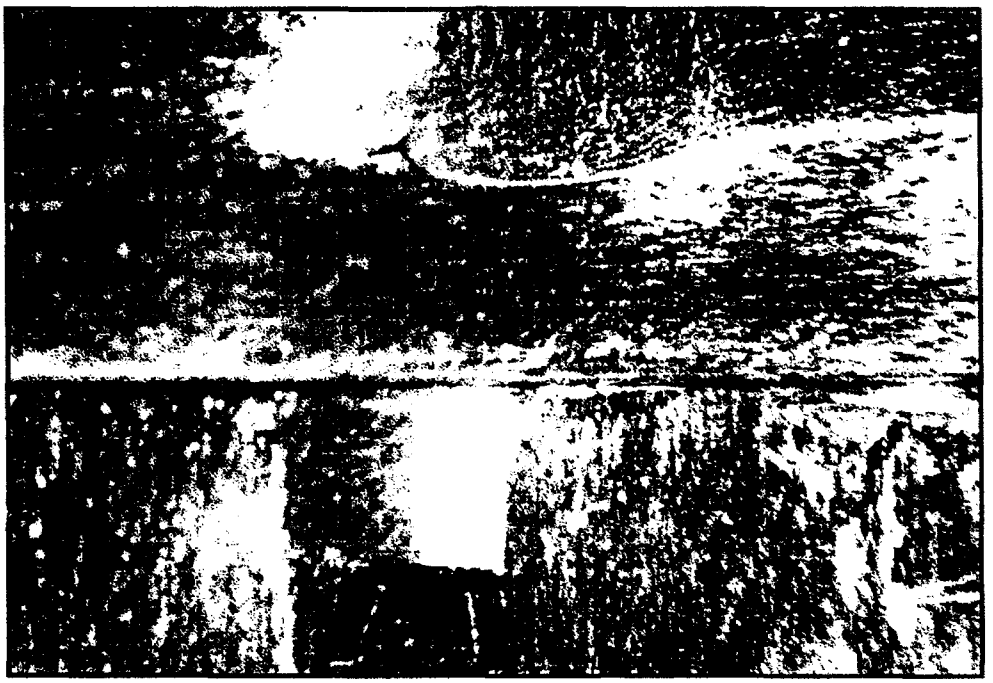

Figure A-39. SAIC Carbon/Carbon, Polished vs. Unpolished, 35x

Figure A-40. SAIC Carbon/Carbon, Polished vs. Unpolished, Edge View

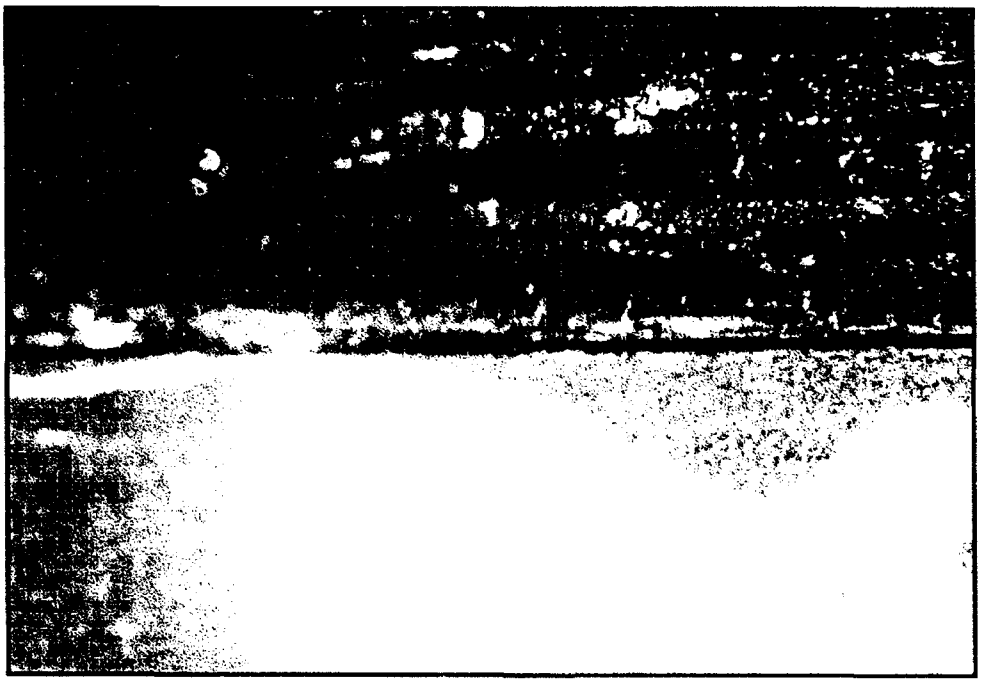

Figure A-41. SAIC Carbon/Carbon, Polished vs. Unpolished, Edge View